Caroline Berge Hansen

In Situ Assessment of a Novel Underwater pCO_2 Sensor Based on NDIR Spectrometry Enclosed in a Semipermeable Membrane for Use in Aquaculture

Evaluation of Four Biofouling Protection Mechanisms

Master's thesis in Analytical Chemistry
Supervisor: Øyvind Mikkelsen
June 2019

Master's thesis

NTNU
Norwegian University of Science and Technology
Faculty of Natural Sciences
Department of Chemistry

NTNU
Norwegian University of
Science and Technology

Caroline Berge Hansen

In Situ Assessment of a Novel Underwater pCO_2 Sensor Based on NDIR Spectrometry Enclosed in a Semipermeable Membrane for Use in Aquaculture

Evaluation of Four Biofouling Protection Mechanisms

Master's thesis in Analytical Chemistry
Supervisor: Øyvind Mikkelsen
June 2019

Norwegian University of Science and Technology
Faculty of Natural Sciences
Department of Chemistry

NTNU
Norwegian University of
Science and Technology

Summary

In Recirculating Aquaculture Systems (RAS), the water quality is mainly determined by metabolites produced and excreted by the fish, and how effectively they are removed from the system. Carbon dioxide (CO_2) is a product of fish metabolism, and can be accumulated in RAS if not removed successfully. High concentrations of CO_2 have been linked to negative impacts on growth performance, welfare, and health of the fish. Thus, the CO_2 level in RAS is an important water quality parameter to monitor.

In this thesis, an in situ method in which a Non-Dispersive Infrared (NDIR) sensor enclosed in a semipermeable membrane was tested in RAS. The studied sensor was recently developed by Pro-Oceanus Inc., and has been designed especially for use in aquaculture industry.

Although materials are designed to minimize biofouling, biofilms will eventually form on the surface when deployed in systems with significant biological activity. This may lead to inaccurate measurements due to decreased permeability of membranes, and macrofouling aggregates altering the local chemical environment. For this reason, four mechanisms to minimize fouling on the sensor membrane were tested.

The tested mechanisms were a polytetrafluoroethylene (PTFE or Teflon) membrane engineered to minimize fouling, a copper grid with biocide properties, a polydimethylsiolxane (PDMS) membrane with graphene oxide (GO) and zinc oxide (ZnO) nanocomposites with enhanced antifouling properties and a water-pumped flow-through head which provide reduced sensor equilibration time with the surrounding water sample and an effective means of preventing biofilms. It was assessed how far fouling on the membrane affected the stability of the sensor signal, and optimized maintenance routines using combinations of cleaning and protection procedures.

Data derived from the Pro-Oceanus Solu-Blu sensor were compared with measurements of CO_2 from classical titration with sodium hydroxide, Franatech solid state electrolyte CO_2 sensor, and CO_2 calculations from Total Inorganic Carbon (TIC), pH, temperature, salinity and experimentally determined dissolution constants.

A dynamic range was captured during a daily cycle when using all antifouling mechanisms except for the pumped head. The reason for this may be that the membrane is sensitive towards particles such as pellets colliding with the membrane and pressure changes when using the pumped head. During testing with the pumped head and the PDMS membrane, water penetrated behind the membrane. Due to few reference measurements, it can not be concluded that the Pro-Oceanus Solu-Blu CO_2 sensor measured the real concentration in the tank or if the measurements were affected by biofouling. Nevertheless, the results indicated that measurements using the Teflon membrane were affected by biofouling.

Sammendrag

I lukkede oppdrettsanlegg med resirkulering av vann (RAS) bestemmes vannkvaliteten hovedsakelig av hvor effektivt vannrensesystemet fjerner metabolitter produsert og utskilt av fisken. Hvis rensesystemet ikke fungerer optimalt, kan metabolitter slik som karbondioksid (CO_2) akkumuleres i systemet. Forhøyede konsentrasjoner av CO_2 har blitt knyttet til redusert ytelse, velferd og helse for fisken. For å sikre et sunt miljø som maksimerer fiskens vekst og helse er det viktig å kontrollere konsentrasjonen av CO_2 i RAS.

En ikke-dispergerende infrarød CO_2-sensor innelukket i en semipermeabel membran ble i denne masteroppgaven testet i RAS. Sensoren var nylig utviklet av Pro-Oceanus Inc. spesielt for bruk i akvakultur.

I systemer med signifikant biologisk aktivitet dannes biofilmer på overflaten av materialer selv om de er designet for å forhindre begroing. Dette kan føre til nedsatt permeabilitet av semipermeable membraner, og endringer i det lokale kjemiske miljøet grunnet makro-organismer. I denne oppgaven ble fire ulike mekanismer for å forhindre begroing på sensorens membran testet: en polytetrafluoretylen (PTFE eller Teflon) membran designet for å redusere begroing, et kobbergitter med biocid egenskaper, en polydimethylsiloksan (PDMS) membran med grafenoksid (GO) og sinkoksid (ZnO) nanokompositter med antibegroingsegenskaper, og et pumpehode som øker sensorens responstid og forhindrer dannelsen av biofilmer på membranen. Det ble studert hvordan begroing påvirket sensorens målinger, samt optimaliserte vedlikeholdsrutiner med en kombinasjon av vaske- og beskyttelsesprosedyrer.

Målingene med Pro-Oceanus Solu-Blu CO_2-sensor ble sammenlignet med verdier fra klassisk titrering av CO_2 med natriumhydroksid, Franatech fast fase elektrolytt-sensor, og beregninger av CO_2 fra total uorganisk karbon, pH, temperatur, og eksperimentelt bestemte dissosiasjonskonstanter.

Daglig CO_2 variasjon ble observed ved bruk av alle mekanismene for å forhindre begoring, unntatt pumpehodet. Dette kan være grunnet sensitivitet mot partikler som kolliderer med membranen og endring i trykk når dette hodet brukes. Vann penetrerte bak sensorens membran under testingen av pumpehodet og PDMS membranen. På grunn av få referansemålinger kan det ikke konkluderes med at Pro-Oceanus Solu-Blu CO_2 sensor målte den reelle konsentrasjonen i vannet, eller om målingene var påvirket av begroing. Allikevel indikerte resultatene at målingene ved bruk av Teflon membranen ble påvirket av begoing.

Preface

This master thesis is written at the Department of Chemistry at the Norwegian University of Science and Technology (NTNU), and is the final product of the Master's degree in "Chemical Engineering and Biotechnology" with specialization in Analytical Chemistry. The thesis is a part of the Sensor project within the CtrlAqua centre for research-based innovation, and marks the end of my 5 years of study at NTNU.

I wish to thank various people for their contribution to this project;

Special thanks should be given to Professor Øyvind Mikkelsen, my research project supervisor, for his professional guidance and valuable support;

The people at Nofima, Sunndaløra, for giving me the opportunity to conduct my study in their facilities. Especially Andre Meriac, my contact person at Nofima, for his engagement and support;

Yuriy Marchenko and May Britt Mørkedal, for valuable technical support on this project;

Bernhard Eckel, for keeping me updated on the sensor status at Nofima when I was not there;

Dag Egil Bundgaard, for conducting the Total Inorganic Carbon (TIC) measurements;

Shazia Aslam, for helping me with statistical analysis;

Syverin Lierhagen, for the execution of the element analysis with ICP-MS;

All my friends and family, for providing me with unfailing support and continuous encouragement throughout my years of study and through the process of researching and writing this thesis;

Lastly, I want to give a thanks to my classmates, Kristin Runde and Torstein Bye, for making studying fun and pushing me to do better.

Contents

List of Tables

List of Figures

Abbreviations

ANOVA	=	Analysis of Variance
CA	=	Carbonate Alkalinity
DLR	=	Dual Lifetime Referencing
FRI	=	Feed Ration Ingested
GO	=	Graphene Oxide
ICP-MS	=	Inductively Coupled Plasma Mass Spectrometry
ISE	=	Ion Selectice Electrode
KHP	=	Potassium Hydrogen Phthalate
mg/L	=	Milligram per Liter
NDIR	=	Non Dispersive Infrared
OFR	=	Oxygen Feed Ratio
PDMS	=	Polydimethylsiloxane
PF	=	Peaking Factor
PP	=	Polypropylene
ppt	=	Parts Per Trillion
PTFE	=	polytetrafluoroethylene or Teflon
PVC	=	Polyvinyl chloride
RAS	=	Recycling Aquaculture Systems
RQ	=	Respiratory Quotient
SEM	=	Scanning Electron Microscope
TA	=	Total Alkalinity
TDGP	=	Total Dissolved Gas Pressure
TFC	=	Thin Film Composites
TIC	=	Total Inorganic Carbon
TPP	=	Tetraphenylporphyrin
TPX	=	Polymethylpene
vpm	=	Volume per Million
ZnO	=	Zinc Oxide
ZPC	=	Zero Point Calibration

Chapter 1

Introduction

Recirculating Aquaculture System (RAS) represent a way to farm fish in a controlled indoor environment. In such systems, the water is filtered and cleaned before it is recycled back to the fish culture tanks to ensure a healthy environment that maximize growth and health. To achieve good water quality, the water treatment system must efficiently remove fish metabolites from the system. The most important metabolites that effect fish are carbon dioxide (CO_2) and nitrogenous components. The metabolism is dependent on various factors, such as fish size and life stage, water temperature, stress, feed intake, and feed composition.

RAS has been in existence, in one form or another, since the mid 1950's. However, only recently, the potential to grow fish on a commercial scale has been realized. New water quality technology, testing and monitoring instrumentation and computer enhanced system design programs have been incorporated and revolutionized the ability to grow fish in culture tanks. The interest in closed systems is also increasing due to challenges in open systems such as fish escape, parasite and pathogen control, mammalian and avian predation, and solid and soluble waste management. In addition, a growing public demand for healthy, tasty, and affordable food is stimulating the fish farming industry. (Chadwick et al., 2010)

In intensive RAS, metabolic derived carbon dioxide (CO_2) can accumulate if there is a lack of degassing processes or limited system water exchange. Elimination of CO_2 through the fish gills is only possible if an adequate CO_2 gradient exists between the fish blood and the surrounding water. An increase in ambient CO_2 partial pressure is rapidly reflected in blood CO_2 in fish, and reduce the capacity of the blood to transport oxygen (O_2) to the cells. Consequences are increased liability to infectious diseases and reduced effectiveness of food intake. (Zosel et al., 2011) Fish can compensate for the reduced pH by excreting H^+ and taking up HCO_3^- from the surrounding water over a period of time. However, there is a limit to these mechanisms which set the upper limit for CO_2 tolerance in fish. (Chadwick et al., 2010) Discussion around the recommended maximum level of CO_2 to maintain welfare and maximum growth of salmonoids exist. Some studies may overestimate the maximum safe level of CO_2 by not being long enough to detect

comparatively small differences in growth rate that could be significant in an aquaculture setting. Further, the toxicity of CO_2 appears to depend on several factors such as life stage, water temperature, and oxygen saturation. Often, precautionary approaches are adopted. In Norway, the safe upper limit of dissolved CO_2 concentration has been set to 15 mg/L. (Good et al., 2018)

A study on the effect of CO_2 on growth performance, welfare, and health of Atlantic salmon post-smolt in brackish RAS showed that the growth significantly decreased linearly with increasing CO_2 in the water. Further, it showed a maximum growth performance at CO_2 concentrations below 12 mg/L in experiments lasting for 12 weeks. The same study showed that fish exposed to 40 mg/L CO_2 presented a thinner skin dermis. Except skin, no major effects of health and welfare were observed in treatments between 5 and 40 mg/L CO_2. (Mota et al., 2019) As research and experience has linked elevated dissolved CO_2 to reduced growth performance, poor feed conversion, and a variety of health issues in farm-raised fish, CO_2 is an important water quality parameter in RAS to provide optimal growth and feed utilization. (Good et al., 2018) (Fietzek et al., 2014) There are several commercially available sensors for dissolved CO_2 monitoring in aquatic environment. Despite this, the experience is that the sensors are known to have several issues such as signal drift, interferences, change in response due to biofilm formation and clogging among other issues.

The Nofima Centre for Recirculation in Aquaculture carries out research on recirculation in aquaculture on a broad basis and was built in 2010. Along with research on recirculation technology, areas of nutrition, physiology, and fish welfare are studied at the centre. It is the only research facility in Norway of approximate commercial size (1750 m^2), and has access to both fresh and seawater. The centre has four separated recirculating systems. Each of these contains side and centre outlets in the tanks, particle collectors at tank level, ozone treatment, micro sieves, moving bed biofilters/bioreactors each with three chambers, counter current carbon dioxide degasser, sump and oxygen treatment. The centre is controlled by several programmable logic controllers which enables continual logging of research data of pump status, water flow, temperature, oxygen, pH and oxidization-reduction potential. The centre also has an auto analyzer for rapid and accurate measurement of ammonia, nitrite, nitrate and CO_2. The research plant is ideal for testing out equipment, methods and operational routines in collaboration with the industry. (Nofima, 2019)

Chapter 2

Theory

2.1 Equilibrium aspects of the carbonate system

Although seawater composition is well defined and dominated by a limited number of major ions, the chemistry is complicated. It involves a variety of different acid-base species in addition to the three forms of carbon dioxide: dissolved carbon dioxide, bicarbonate ion, and carbonate ion.

Gaseous CO_2 dissolves in water according to Henry's law of solubility presented in Equation (2.1). This law only applies for dilute, ideal solutions where the liquid do not react with the gas being dissolved. The solubility coefficient, k_H, is dependent on temperature and salinity. pCO_2 is the partial pressure of dissolved CO_2. (Pedersen, 2018) When carbon dioxide dissolves in water, it hydrates to yield carbonic acid, H_2CO_3, which rapidly dissociates into bicarbonate (HCO_3^-) and carbonate (CO_3^{-2}) ions. The hydration of carbon dioxide is slow compared to the ionisation of H_2CO_3 which makes it possible to distinguish between dissolved carbon dioxide (CO_2 (aq)), and hydrated species.

$$xCO_2 = \frac{pCO_2}{k_H} \tag{2.1}$$

At equilibrium, the concentration of carbonic acid is only about 1/1000 of the concentration of dissolved carbon dioxide, and has no special significance for the acid-base equilibria since both are uncharged. The carbonate system is described by four equilibrium reactions shown in Equation (2.2), Equation (2.3), Equation (2.4) and Equation (2.5) and their corresponding equilibrium constants K, K_0, K_1 and K_2. (Dickson, 2010) (Zeebe and Wolf-Gladrow, 2001)

$$\mathrm{CO_2\,(g)} \overset{\mathrm{K}}{\rightleftharpoons} \mathrm{CO_2(aq)} \tag{2.2}$$

$$\mathrm{CO_2\,(aq) + H_2O\,(l)} \overset{\mathrm{K_0}}{\rightleftharpoons} \mathrm{H_2CO_3(aq)} \tag{2.3}$$

$$H_2CO_3(aq) \overset{K_1}{\rightleftharpoons} H^+(aq) + HCO_3{}^-(aq) \tag{2.4}$$

$$HCO_3{}^-(aq) \overset{K_2}{\rightleftharpoons} H^+(aq) + CO_3{}^{2-}(aq) \tag{2.5}$$

It is difficult to analytically distinguish between the two electrically natural species CO_2 (aq) and H_2CO_3 (aq), and they are therefore often grouped together and expressed as the sum concentration of a hypothetical species, CO_2* (aq). Redefining Equation (2.2), Equation (2.3) and Equation (2.4) gives

$$CO_2(g) \overset{K_0{}^*}{\rightleftharpoons} CO_2{}^*(aq) \tag{2.6}$$

$$CO_2{}^*(aq) + H_2O(l) \overset{K_1{}^*}{\rightleftharpoons} H^+(aq) + HCO_3{}^-(aq) \tag{2.7}$$

The dissociation constants K_0*, K_1* and K_2 are defined by Equation (2.8), Equation (2.9) and Equation (2.10). f(CO_2) is the fugacity of carbon dioxide in the gas phase and brackets represent total stoichiometric concentrations of the particular chemical species enclosed. These equilibrium constants vary with temperature, pressure and salinity of the solution. pK is defined as the logarithm of the dissociation constant K. (Dickson et al., 2007)

$$K_0{}^* = [CO_2{}^*]/\,f(CO_2) \tag{2.8}$$

$$K_1{}^* = [H^+][HCO_3{}^-]/\,[CO_2{}^*] \tag{2.9}$$

$$K_2 = [H^+][CO_3{}^{2-}]/\,[HCO_3{}^-] \tag{2.10}$$

There is an inverse exponential relationship between CO_2 partial pressure and water pH. An addition of CO_2 to the water will affect the carbonate-equilibrium and result in a reduced water pH. The solubility of CO_2 is inversely proportional to increasing temperature and salinity. More CO_2 will dissolve with a lower temperature and salinity, resulting in a lower pH. (Chadwick et al., 2010) Figure 2.1 shows a plot of the carbonate system and how the relative proportions of CO_2*, $HCO_3{}^-$ and $CO_3{}^{2-}$ control pH, and how temperature (T), pressure (P) and salinity (S) effect the equilibrium. The reference case (solid line) is T=25° C, S=35 ppt, and P=1 atm. pK_1=5.86 and pK_2=13.22 for the reference case. (Zeebe and Wolf-Gladrow, 2001)

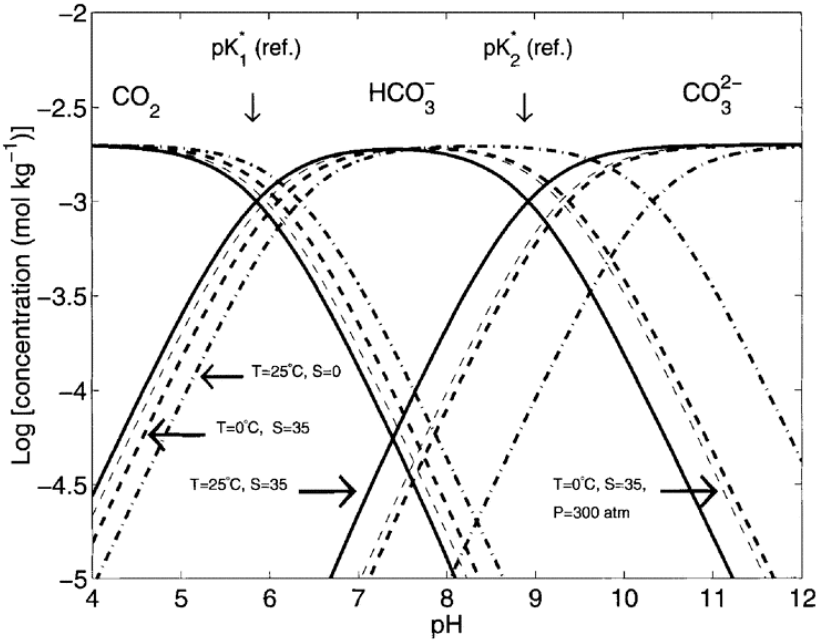

Figure 2.1: A plot of the carbonate system showing how the relative proportions of CO_2*, HCO_3^- and CO_3^{2-} control pH in sea water. The reference case (solid line) is T=25° C, S=35 ppt, and P=1 atm. (Zeebe and Wolf-Gladrow, 2001)

Alkalinity

Alkalinity is an important and useful concept in the context of the carbonate system in seawater. Total Alkalinity (TA) measures the ability of a solution to neutralize acids to the equivalence point of carbonate or bicarbonate, and is equal to the stoichiometric sum of the bases in solution as shown in Equation (2.11). Minor components includes species such as HPO_4^{2-} and $H_2SIO_4^-$, and is in very small concentrations in typical seawater pH values around 8. The carbonate alkalinity, CA, is a simplification of TA and is given by Equation (2.12). (Zeebe and Wolf-Gladrow, 2001)

$$TA = [HCO^{3-}]+2[CO_3^{2-}]+[B(OH)_4^-]+[OH^-]-[H^+]\pm minor\,components \quad (2.11)$$

$$CA = [HCO_3^-] + 2[CO_3^{2-}] \quad (2.12)$$

Total Inorganic Carbon (TIC)

Total inorganic carbon (TIC) is the sum of concentration of the three coexisting species: bicarbonate ion, carbonate ion and unionized dissolved carbon dioxide as seen in the equation below. TIC can be measured directly in a water sample by acidifying the sample to convert carbonate and bicarbonate to carbon dioxide. The carbon dioxide diffuses trough a gas permeable membrane into a weakly buffered phenolphthalein indicator solution and causes the indicator to become more acidic. A more acidic solution results in a loss of color proportional to the concentration of CO_2, and are thus possible to quantify by using a calibration curve and a suitable detector.

$$TIC = [CO_2^*] + [HCO_3^-] + [CO_3^{2-}] \tag{2.13}$$

2.1.1 Calculation of dissolved carbon dioxide

The concentrations of the individual species of the carbon dioxide system can not be measured directly. However, the various equilibrium and mass-balance equations that describe the acid-base chemistry of seawater compromise a set of equations with a limited number of linearly independent variables. It is possible to obtain a complete description of the acid-base composition of a sample at a particular temperature and pressure provided any two of the four measurable parameters: pH, Total Alkalinity (TA), fugacity of carbon dioxide (fCO_2) and Total Inorganic Carbon (TIC). Constants for other acid-base species in the water and dissociation constants of carbonic acid are also needed to calculate the components of the CO_2 system from these measurements.

At Nofima, the dissolved carbon dioxide concentration is calculated by measuring pH, temperature, salinity, and TIC while using experimentally determined values for the dissociation constants. The equations to determine the logarithmic dissociation constants, pK_1 and pK_2 are shown in Equation (2.14) and Equation (2.15). S is salinity in ppt, TIC is in mmol/L and T is temperature in K. The field measurements to determine these constants were performed in surface and deep waters from the Atlantic, Indian, Southern and Pacific oceans where the contribution from organic acids were assumed to be negligible. (Millero et al., 2002)

$$pK_1 = -8.712 - 9.460 \cdot 10^{-3} \cdot S + 8.56 \cdot 10^{-5} \cdot S^2 + \frac{1355.1}{T} + 1.7976 \cdot ln(T) \tag{2.14}$$

$$\begin{aligned} pK_2 = 17.0001 - 0.01259 \cdot S - 7.9334 \cdot 10^{-5} \cdot S^2 + \\ \frac{936.291}{T} - 1.87354 \cdot ln(T) - \frac{2.61471 \cdot S}{T} + \frac{0.07479 \cdot S^2}{T} \end{aligned} \tag{2.15}$$

The dissociation constants, K_1 and K_2 are found by the following equations. ρ is the water density.

$$K_1 = 10^{-\frac{pK_1 \cdot 1000}{\rho}} \tag{2.16}$$

$$K_2 = 10^{-\frac{pK_2 \cdot 1000}{\rho}} \tag{2.17}$$

By using TIC, K_1, K_2 and $[H^+]$, the concentration of HCO_3^- can be determined:

$$[HCO_3^-] = \frac{TIC}{\frac{[H^+]}{K_1} + \frac{K_2}{[H^+]} + 1} \tag{2.18}$$

The concentration of carbon dioxide, c_{CO_2}, in μg/L can be calculated by the following equation. M_{CO_2} is the molar mass of CO_2.

$$c_{CO_2} = \frac{[H^+][HCO_3^-]}{K_1} \cdot M_{CO_2} \tag{2.19}$$

2.2 Principles for measuring dissolved carbon dioxide

Carbon dioxide sensors are used in various applications such as in environmental control, biotechnology, biology, medicine, aquaculture, and food industry. Knowledge of the basic detection principles and the windows for their applications is necessary to find the appropriate technology to be applied for measuring dissolved CO_2. Depending on the medium in which CO_2 needs to be measured and the requirements for measuring range, accuracy, long-term stability, selectivity, and maintenance, different methods can be applied. In this section, some methods for measuring dissolved CO_2 will be presented. (Zosel et al., 2011)

Although the sole measurement of pCO_2 is not sufficient to fully characterize the aquatic CO_2 system, it is a determining factor for air-water gas exchange and responds to biogeochemical processes such as photosynthesis and respiration. In aquaculture, levels of CO_2 should be expressed as partial pressure because most of the CO_2 produced by fish diffuses across the gills down a partial pressure gradient from plasma to water. However, since the concentration of CO_2 is directly proportional to its partial pressure, levels of CO_2 is commonly given in mg/L. (Chadwick et al., 2010)

2.2.1 Non Dispersive Infrared (NDIR)

Infrared detection method

Non Dispersive Infrared (NDIR) detection is one of the most common types of sensors used to measure carbon dioxide (CO_2), and provides accurate determination of CO_2 at both low and high concentrations. The technique uses the fact that the IR spectrum of each molecule is unique. In a typical NDIR probe for CO_2 measurement, an IR lamp produce a 4.2 micron band of IR radiation and direct the waves of light through a tube filled with a sample of air towards the IR light detector. This exact band width is absorbed by CO_2 molecules present in the sample. Further, an optical filter absorbs every wavelength of light except the wavelength absorbed by CO_2. The IR detector reads the amount of light that was not absorbed by the CO_2 molecules or the optical filter. This corresponds to the difference between the amount of light radiated by the IR lamp and the amount of IR light received by the detector, and is proportional to the number of CO_2 molecules in the air inside the tube. The most common detectors in NDIR sensors are pyroelectric sensors and thermopiles. (Zosel et al., 2011) Schematic setup of a multi-spectral NDIR gas sensor for two gases is shown in Figure 2.2.

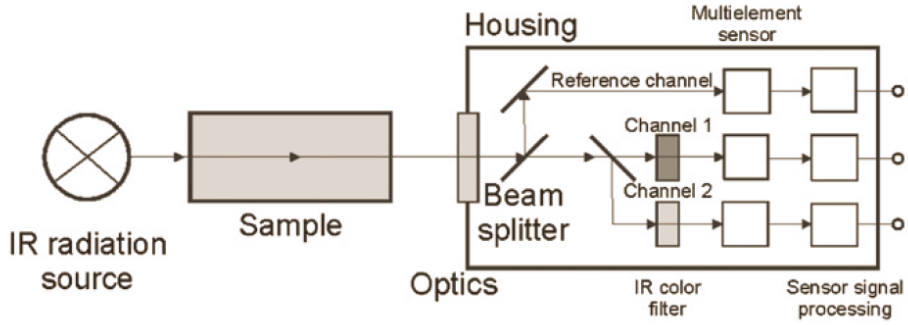

Figure 2.2: Schematic setup of a multi-spectral NDIR gas sensor for two gases. (Zosel et al., 2011)

The underlying physical principles of NDIR sensor gas detection provide a measure of the number of molecules of a specific gas. In order to accurately calculate the partial pressure of CO_2, p_{CO_2}, the total gas pressure, P, and ratio of CO_2 molecules versus the total number of molecules, x_{CO_2}, must be known. (Atamanchuk et al., 2014) A pressure sensor within the detector cell determines the pressure which is used to internally correct CO_2 measurements. Input salinity values provide automatic salinity correction.

$$p_{CO_2} = P \cdot x_{CO_2} \tag{2.20}$$

The NDIR unit is temperature stabilized within the sensor because temperature changes in the detector cell will affect the accuracy of the measurement if not appropriately corrected. As gas molecules are heated, their velocities increase, leading to an apparent increase in the number of gas molecules in a given volume by a NDIR detector. To prevent condensation within the sensing cell, an internally stabilized gas detector cell temperature is held at a temperature above the surrounding water temperature. (Pro-Oceanus, 2016)

To prevent signal drift, an automatic zero compensation function may be added which periodically removes CO_2 from the system and records a new zero CO_2 baseline. The optical unit may combine a two beam setup with repeated Zero Point Calibration (ZPC). The two-beam setup use a reference channel, which measures the intensity at a wavelength that is not exciting CO_2 vibrations, to correct drift. ZPC operates by circulating the internal gas through a CO_2 absorption chamber containing soda lime or Ascarite. Signal drift can be caused by contamination of the optical cell, optical source aging, and changes in detector sensitivity.

The sensor is calibrated at a known optical cell temperature and pressure against standard gasses of xCO_2 (mole fraction of CO_2 in dry air). Calibration can be obtained by least-squares fitting, and tested by measuring known mixtures of CO_2. While the calibration equation provides a raw xCO_2 from the IR measurements, empirical corrections are applied to account for the differences of conditions between calibration and measurement (temperature, pressure, and water vapor). (Jiang et al., 2014)

Equilibration dynamics and instrument response time

Dissolved carbon dioxide (CO_2) sensors using NDIR technology measure CO_2 in gas phase that is in equilibrium with surrounding water. A semipermeable pressure-resistant membrane is used to achieve mass transport of gas between the gaseous headspace of the sensor and the surrounding water. This process require diffusion of molecules from the liquid across the semipermeable membrane to the gaseous headspace of the sensor and back. Several factors affect the time it takes to equilibrate the gas headspace with the surrounding liquid through a semipermeable membrane.

There is a finite time required for the shift between the dissolved and gas phase of a molecule due to kinetics of solubility. The rate is dependent on temperature and salinity, and to a small degree, pressure. The membrane can be described using the Laws of Diffusion, where the diffusion coefficient of the semipermeable membrane is a function of the gas solubility coefficient in the membrane and the permeability of that gas through the membrane.

The equilibration rate of diffusion processes is often measured in terms of a time constant, t_{63}. This constant represents the time it takes to reach 63 $\%$ of equilibrium. The flux of gases across a membrane is a function of the concentration gradient between either side of the membrane. For example, if the concentration difference of CO_2 in the sensor headspace and the surrounding water is large, the gas flux across the membrane will be rapid. As a gas moves across the membrane into or out of the gas headspace, the concentration gradient decreases. As a result, the rate of the gas flux across the membrane reduces. The concentration gradient across the membrane continually changes, and the resulting change in concentration of a particular gas in a headspace can be described mathematically as a logarithmic function.

Advection is a rapid process, and transfer the dissolved gas near the membrane surface. Diffusion of gas through the water boundary layer is the rate limiting factor in the transfer from the water to the outer surface of the semipermeable membrane. Temperature has a major effect on the diffusion rate. An increased temperature improve the response time of the sensor, while cooler waters slow the process. The water-side boundary layer plays an important role in the response time of the sensor. The thickness of the layer can vary, and as a result, so does the time to diffuse through the boundary layer. The thickness is determined by the hydrodynamics next to the membrane surface. Stagnant water will produce the thickest boundary layer, resulting in the slowest response time. An increased water velocity will reduce the boundary layer thickness in addition to reduce the potential for biofouling. At low water velocities, slow equilibrium time may result in under-reading of the gas measurement. However, given enough time to equilibrate, the sensor will provide accurate readings. A water-pumped flow-through head provide faster equilibration time and improved antifouling of the semipermeable membrane by increasing the water velocity near the membrane. (Pro-Oceanus, 2016)

The semipermeable membrane is normally composed of a mono-layer of a polymer such as polydimethlysiloxane (PDMS) or polytetrafluoroethylene (PTFE or Teflon) with an effective layer thickness of around 10 μm. The semipermeable membrane allows gases to penetrate into the sampling volume while resisting the penetration of external liquid and sustaining the hydrostatic pressure so that it does not collapse the sampling volume. The thickness of the membrane plays an important role in the time for equilibration. A thinner

membrane results in higher permeability and shorter response time. Beside the membrane, the overall design of the sensor, such as tube volume and tubing material, influences the response time. (Fietzek and Körtzinger, 2010) Biofilms forming on the membrane will lead to a slowdown of the equilibrium rate due to decreased permeability of the membrane, and the production of CO_2 by organisms of the biofilm can result in erroneous data. Regular cleaning can minimize this effect. Gas bubbles entrapped during deployment or formed in situ may cause inaccurate data if they are accumulated on the membrane interface. This may be prevented by placing the instrument in a horizontal position to allow release of gas bubbles.

If the membrane is not fully compressed against it support, an elevated total dissolved gas pressure may build up inside the gas stream where CO_2 is measured. While the detector compensates for changes in gas pressure, measurements may not be within the specified accuracy while this excess is released via diffusion through the membrane. Gas pressure buildup on the gas side of the membrane can result in bulging of the membrane when removed from immersion. (Pro-Oceanus, 2016)

Currently, there is an abundance of NDIR CO_2 sensors available in the market. The Solu-Blu CO_2 sensor from Pro-Oceanus Inc. is designed for long term submersion and continuous in situ monitoring of dissolved CO_2 levels. It is suitable for aquaculture monitoring across recirculating systems, live transport, and open pen cages among others. (Pro-Oceanus, 2018)

2.2.2 Standard carbon dioxide titration

Even though standard titration is a typical field method for measuring dissolved CO_2 in aquaculture systems, it only provides an approximation of the dissolved CO_2 concentration in a water sample. Both sodium hydroxide and hydrochloric acid may be used as titrant, depending on the sample solution. In the hydroxide method, a phenolftalein indicator is added to the sample to identify the titration endpoint. If color or turbidity makes it difficult to see the color change at the endpoint, the indicator solution can be replaced by a pH probe. Carbonic acid formed by carbon dioxide in the sample is titrated with a sodium hydroxide standard solution until the indicator changes color at the endpoint of 8.3. If hydrochloric acid is used as titrant, the endpoint is 4.3. The amount of acid or base added is measured and a calculation is made to determine the CO_2 content of the water sample. Analysis of the sample should be performed at the time of sampling in order to prevent changes in the CO_2 concentration. A decrease in CO_2 concentration may come from CO_2 being lost from the solution during transit and storage. The samples need to be filtered if particulates are present that may contain carbonates. This is due to solution of finely divided carbonates such as calcium carbonate can be a result of temperature or pressure changes, and increase the CO_2 concentration in the sample. (Hach, 2015)

Aquaculture water, tap water, seawater and water from lakes, rivers etc. all contain substances that interfere with this method to some degree. Cations and anions that disturb the normal CO_2-carbonate equilibrium will interfere with both the hydroxide and hydrochlorid titration. In the hydroxide method, any source of acidity other than CO_2 will cause a false positive result. In addition, metal ions that precipitate in alkaline solution (e.g. aluminum, chromium, copper, iron) can also result in a false positive result. (CHEMetrics, 2012) In waters of high organic loadings, such as in aquaculture systems, there are numer-

ous substances that can affect the alkalinity, including tannic and fulvic acids, amino acids, fatty acids, sulfides, phosphates and ammonia. (Moran et al., 2010) (Wolf-Gladrow et al., 2007) In addition, other weak acids that may interfere are boric acid, hydrogen sulphate, silicate, phosphoric acid and its product by dissociation, ortosilicic acid, nitrous acid, and hydrofluoric acid.

Ammonia is the end product of protein catabolism in fish, and is eliminated from the blood upon passage through the gills. (Randall and Wright, 1987) In aqueous media, the chemical equilibrium between ammonia and ammonium is dependent on pH as can be seen in Figure 2.3. At pH 7, which is the average pH in the studied RAS tank, ammonium is the prevalent specie, and may interfere with the hydroxide method. (Turley et al., 2004)

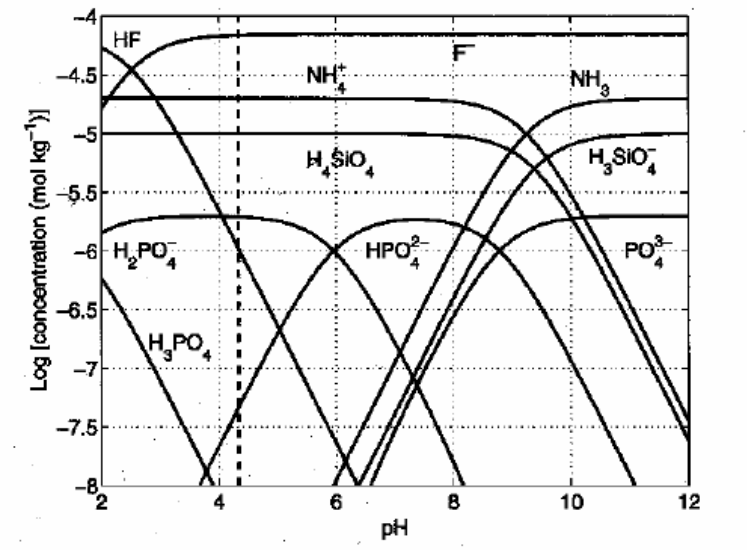

Figure 2.3: Changes in speciation of phosphate, silicate and ammonia with pH. (Turley et al., 2004)

Preparation of the standard hydroxide solution

For the standardization of the sodium hydroxide (NaOH) solution used for standard titration, potassium hydrogen phatalate (KHP) may be used a primary standard. The reaction is shown in the following equation. (Banica, 2015)

$$\mathrm{KPH} + \mathrm{OH}^- = \mathrm{KP}^- + \mathrm{H_2O} \tag{2.21}$$

The concentration of the NaOH solution is determined by Equation (2.22). V_{NaOH} is the equivalence volume in liter. n, m and M is the number of moles, mass and molar mass of the compound in subscript respectively.

$$c_{NaOH} = \frac{n_{NaOH}}{V_{NaOH}} \tag{2.22}$$

where

$$n_{NaOH} = n_{KHP} = \frac{m_{KHP}}{M_{KHP}} \tag{2.23}$$

The concentration of carbon dioxide in mg/L in the sample is determined as shown in Equation (2.24). c_{NaOH} is the concentration of the NaOH standard solution, V_{NaOH} is the volume of the NaOH solution used in the titration, M_{CO_2} is the molar mass of carbon dioxide and V_{sample} is the volume of the water sample in liters. The number 2 in the denominator is due to the relationship c_{CO_2}:c_{NaOH} = 1:2.

$$c_{CO_2} = \frac{c_{NaOH} \cdot V_{NaOH} \cdot M_{CO_2} \cdot 1000}{V_{sample} \cdot 2} \tag{2.24}$$

2.2.3 Solid state carbon dioxide sensors

Electrochemical cells based on solid electrolytes operate at high temperatures, and have been manufactured and applied for a long time. The cells may work potentiometrically according to Nernst equation or in columetric mode according to Faraday's law. The sensors can measure a long period of time without calibration and display rapid response times. The solid electrolyte used for such cells is oxide ion conductors.

Potentiometric determination of CO_2 is possible if electrochemical equilibrium between the ions of solid electrolytes, CO_2, and electrons in the electrode can be established. Solid alkali carbonates are solid electrolytes at temperatures above 300 °C because the charge carriers, the alkaline ions, are mobile via alkali ion vacancies. By doping, the mobility and thus, the electrical conductivity can be enhanced. In Figure 2.4, a cell consisting of sintered gas-tight sodium carbonate covered on both sides with gold layers to separate the sample gas chamber and the reference gas chamber can be seen. With such solid carbonates, Nernstian gas concentrations cells can be built up and the cell voltage depends on both the concentration of CO_2 and O_2.

Reaction at the working and reference electrode for this cell can be seen in Equation (2.25) and Equation (2.26) respectively. Charge compensation occur by migration of sodium ions from the side having lower CO_2 and O_2 concentration, to the side with higher concentration. This results in sodium carbonate are formed on the side with high gas concentration and disappears on the side with low gas concentration when current flows. The main problem with this method is that pressed alkali carbonates are often hygroscopic and tend to sublimate. This may result in porous electrolytes which diminish the contact between gold, carbonate and gas. (Zosel et al., 2011)

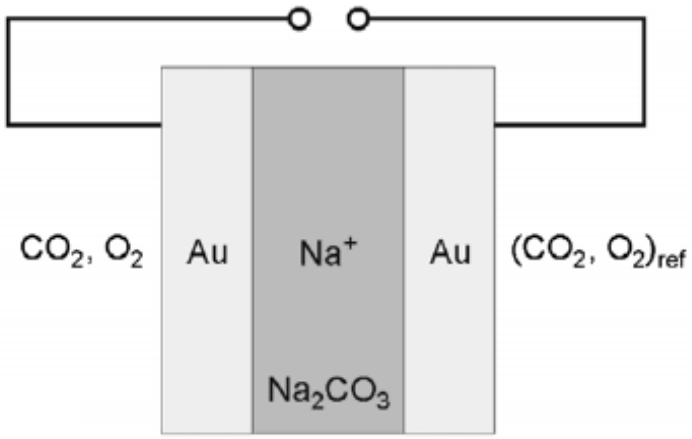

Figure 2.4: Electrochemical cell consisting of sintered gas-tight sodium carbonate covered on both sides with gold layers to separate the sample gas chamber and the reference gas chamber. (Zosel et al., 2011)

$$CO_2(g) + \frac{1}{2}O_2(g) + 2e^-(Au) \longrightarrow CO_3^{2-}(s) \tag{2.25}$$

$$CO_3^{2-}(s) \longrightarrow CO_2(g) + \frac{1}{2}O_2(g) + 2e^-(Au) \tag{2.26}$$

Another example of a solid state CO_2 detector is a thin film based on $BaTiO_3 - CuO$ as a sensitive material. The presence of carbonate groups are responsible for a reversible reaction in the sensing mechanism which change the properties of the material. By measuring the impedance of the material, the CO_2 concentration can be found. (Herrón et al., 2009)

$$CaCO_3 + H_2O + CO_2 \rightleftharpoons Ba(HCO_3)_2 \tag{2.27}$$

Franatech carbon dioxide sensor

The Franatech sensor measures partial pressure of CO_2 which is equilibrated with the water outside of a semipermeable membrane. The detection technique is based on solid-state electrolyte cell and a gas extraction chamber. (Reggiani et al., 2014) Further information is proprietary.

The output of the Franatech sensor is given in volume per million (vpm), and is converted to mg/L CO_2 by the following equation. M is molar mass of CO_2, T is temperature, and vpm is the output of the Franatech sensor.

$$c_{CO2} = \frac{vpm \cdot M_{CO_2}}{29.41e^{-2400\frac{1}{273+T}-\frac{1}{298}} \cdot 1000} \tag{2.28}$$

2.2.4 Electrochemical carbon dioxide sensors

Electrochemical CO_2 sensors according to the Severinghaus principle have been manufactured and applied for a long time. Due to a simple setup, the sensor involves low costs. A typical CO_2 sensing electrode is shown in Figure 2.5. In such electrodes, the CO_2 partial pressure is determined by measuring the pH value of a bicarbonate solution which is separated from the surrounding gaseous or liquid medium by a semipermeable membrane. Typical membrane materials are polytetrafluorethylene (PFTE), polymethylpene (TPX), silicone and polypropylene (PP) with a thickness between 5 and 30 μm. (Zosel et al., 2011) The dissolved CO_2 diffuses through the semipermeable membrane until an equilibrium is reached between the partial pressure of CO_2 in the sample solution and the CO_2 in the internal filling solution. Diffusion across the membrane affects the level of hydrogen ions in the internal filling solution, and the partial pressure of CO_2 in the sample will be proportional to the concentration of carbon dioxide.

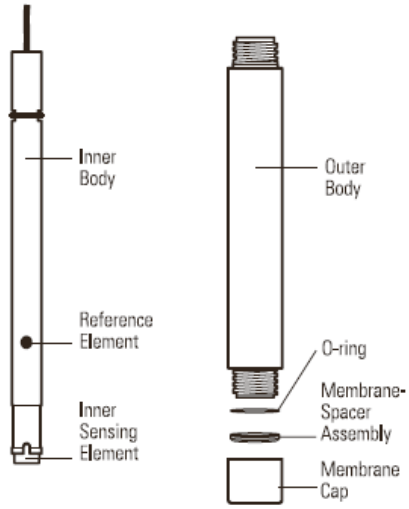

Figure 2.5: A typical electrochemical CO_2 sensing electrode. The inner body is placed inside of the outer body. (ThermoFisherScientific, 2008)

A pH electrode located behind the membrane measures the the hydrogen level of the internal filling solution. This solution contains a high level of sodium bicarbonate which is considered to be constant. The potential of the pH sensing element is related to the hydrogen ion concentration by the Nernst equation. E is the measured electrode potential, E_0 is the reference potential, $[H^+]$ is the hydrogen ion concentration, and S is the electrode slope which is defined as the change in millivolts with every tenfold change in concentration.

$$E = E_0 + S \cdot log[H^+] \tag{2.29}$$

Since the hydrogen ion concentration is directly related to carbon dioxide concentration, electrode response to carbon dioxide is also Nernstian. The reference potential, E_0,

is partly determined by the internal reference element that response to the fixed level of chloride in the internal filling solution.

$$E = E_0 + S \cdot log[CO_2] \tag{2.30}$$

Volatile weak acids may interfere with the determination, and under normal operating conditions, the accuracy of pH probes is reported to be $\pm$ 0.1 pH units or greater. (Moran et al., 2010) Samples and standards should be at the same temperature as temperature changes give rise to errors. Water can diffuse across the membrane as water vapor, and change the concentration of the internal filling solution, resulting in electrode drift. This can be prevented if the ionic strength and temperature of the sample and internal filling solution are the same. (ThermoFisherScientific, 2008)

2.2.5 Optical carbon dioxide sensors

Fiber optic carbon dioxide sensors

Several fiber optic based techniques are available for carbon dioxide detection. Some techniques are based on luminiescence intensity changes of tetraphenylporphyrin (TPP) due to absorption change of a pH indicator dye. However, configurations using indicator dyes suffer from leaching and photobleaching effects. CO_2 could also be measured using direct spectroscopy at 1.75 μm with a sensor based in quartz glass multimode fiber, but this approach needs relatively long interaction lengths and is very sensitive to contamination of the fiber surface.

The combination of optical fiber technologies with the development of new sensitive membranes has greatly contributed to the progress of optical chemical sensors. A hydrogel based sensitive layer whose index depends on CO_2 concentration combined with fiber optic based refractrometric probes can be used to measure CO_2 concentration. The sensitive layer can be based on acid-base equilibrium of phenol and its derivative p-nitrophenol. In the presence of CO_2, hydrogen carbonate is formed which partly protonate the phenols. The hydroxylic group is involved in protolytic reactions that modify the charge distribution in the molecule and a change in refractive index is due to the localization of electrons in the aromatic ring of these compounds. (Gouveia et al., 2010)

Fluorescence based carbon dioxide sensors

Dissolved CO_2 can be measured based on pH change induced by diffusion of CO_2 gas into a pH sensitive Dual Lifetime Referencing (DLR) material which is embedded in a hydrophobic matrix in the form of a thin foil. The sensing foil are composed of two fluorescence indicators embedded in an ion-impermeable, hydrophobic and gas permeable layer that is coated onto a thin film of polyester or glass support. One of the indicators responds to change in the surrounding pH by exhibiting a change in intensity of blue light induced fluorescence. Fluorescence measurements are susceptible to factors such as variations in the background light and excitation intensity. Therefore, the second foil is used as a reference. Its fluorescence excitation and emission spectra overlap significantly with those of the first indicator, but the fluorescence intensity is independent of pH. The combined intensity of the two fluorescence processes lags from the excitation signal by phase

ϕ_{DLR}. This phase is dependent on the relative fluorescence intensities of the two dyes, but since only one of them has a fluorescent intensity dependent on pH, measurements of the phase can be used to detect CO_2. The fluorescence light is detected by a photodiode fitted with a long pass filter to exclude light from the excitation LED and is temperature compensated.

Bleaching of the sensor films and drift in the electronics related to high frequency sampling can induce errors in the measurements. The measuring principle, implies cross sensitivity to any acidic or basic gases and/or vapors. Acetic acid vapors quickly damage the sensor irreversible due to their acidic nature, and dissolved hydrogen sulphide gas poison the sensing foils irreversible. Calibration of this type of sensor is challenging and time consuming, and the response time is 5 minutes in cold water. The power consumption is low in comparison to most other in situ CO_2 sensing systems. (Atamanchuk et al., 2014)

2.2.6 Overview of some carbon dioxide measuring principles

An overview of response time, accuracy, long term stability and price in addition to pros and cons for NDIR, solid state, fluorescence and electrochemical detectors for measuring CO_2 is presented in Table 2.1. (Stiller et al., 2014)

Table 2.1: Response time, accuracy, long term stability and price in addition to pros and cons for NDIR, solid state, fluorescence and electrochemical detectors for measuring CO_2. (Stiller et al., 2014)

	NDIR	**Solid state**	**Fluorescence**	**Electrochemical**
Response time [min]	≥ 5	≥ 15	≥ 6	≥ 8
Accuracy [$\pm$ %]	≥ 1	≥ 2	≥ 2	≥ 2
Long term stability [days]	≤ 365	≥ 365	≤ 183	≤ 5
Price [€]	≥ 2000	≥ 7000	≥ 2000	≥ 400
Cons	Calibration	Expensive, slow	Cross sensitive to H_2S	Work intensive
Pros	Accurate, variable measuring systems	Drift-free	Low energy consumption	Cheap

2.3 Estimating carbon dioxide production rate

Most water quality parameters are not constant in aquaculture. Carbon dioxide and pH concentrations fluctuate or cycle daily due to processes such as respiration and photosynthesis. Animal species are usually active at a specific time of the daily cycle. They are either diurnal, nocturnal or crepuscular, which means that the behavior is characterized by activity at day, night or twilight respectively. Activity, as a prime user of energy, will have a marked effect on oxygen consumption, and thus carbon dioxide release in fish. (Metcalfe et al., 1998)

It is shown that young salmon show diurnal variations in their feeding activity. Both parr and smolt show a nocturnal depression in feeding activity, and it is probable that the fish are habituated to sleep during the hours of darkness when food is less likely to be available. They feed somewhat less from 1 to 2 hours after sunset until 2 or 3 hours after sunrise, and feed in a lower intensity in the evening than during the early morning hours. In addition, there is a somewhat smaller and less consistent mid-day depression in the amount of food taken. If the fish required much food and were very hungry (as in smolt), the depression was not evident. On the other hand, fish with a lower rate of metabolism (as in parr) showed this depression factor. (Hoar, 1942)

Based on stoichiometry of the chemical reactions involved in the metabolism of carbohydrates, one mole of CO_2 is produced when one mole of O_2 is consumed. This results in a Respiratory Quotient (RQ) of unity, but this varies with the substrate metabolized. When RQ is unity, the consumption of 1 g of oxygen should produce 1.375 g of CO_2. This can be used to estimate the carbon dioxide production rate (kg/interval/m^3) in a culture tank. As a thumb rule, each unit of feed will require 0.25 unit of oxygen for fish metabolism although usage rates will depend upon several factors, mainly the type of fish considered. (Timmons and Ebeling, 2007) The daily CO_2 production rate can be estimated using the above information, total feed ration ingested, oxygen feed ratio, a peaking factor and the tank volume as presented in Equation (2.31). FRI is Feed Ration Ingested in kg feed/day, OFR is Oxygen Feed Ratio in kg O_2 consumed/kg feed ingested, PF is a factor used to account for increase in oxygen consumption following feeding and V is the tank volume. By dividing by the daily water flow, F, instead of the tank volume, daily increase of CO_2 in the tank can be estimated. (Chadwick et al., 2010)

$$CO_2production = \frac{FRI \cdot OFR \cdot PF \cdot 1.375}{V} \tag{2.31}$$

2.4 Biofouling

Biofouling is the colonization of an interface by a diverse array of organisms and is a complex natural phenomenon where much remains to be understood. The biofouling development depends on several physical and chemical factors, such as temperature, conductivity, pH, dissolved oxygen content and organic material content. (Delauney et al., 2010) Surfaces are firstly fouled by microbial organisms such as diatoms, hydroids, algal spores and marine bacteria, followed by macroorganisms which include algae. (Cronin et al., 1999) Characteristics and types of affected materials are extremely diverse, ranging from hard plastics such as PVC, soft plastics like nylon and various metals such as steel which may

have flat, smooth or heterogeneous surfaces. The affected surfaces can be mobile such as boats or stationary such as cage structures. The high variability in types of material and their surface characteristics influences the accumulation of fouling species and leads to different fouling assemblages even in the same aquaculture system. Hence, antifouling strategies need to be adapted to the high diversity of materials and fouling organisms present at the given site. (Dürr and Thomason, 2009)

In aquaculture, biofouling may affect equipment, infrastructure, and even the stock, and are maintained at a high level due to leftover fish food and feaces. If instruments are affected, sensor measurements can be disrupted in less than a week. Biofouling can change the biological or chemical properties of the studied site by containing bacteria and algae which are autotrophs or heterotrophs. Autotrophs use photosynthesis to produce organic matter from water, CO_2 and a small number of inorganic nutrients, and heterotrophs produce CO_2 in the metabolic process. (Morrissey et al., 2016) For example if the sensor is set up to measure CO_2, its measurements can be affected by macro-fouling aggregates that alter the local CO_2 concentration. Even if the instrument is engineered to minimize biofouling, biofilms will slowly develop on the surface of the membrane under operation. If the instrument readings is dependent on a semipermeable membrane, biofouling may lead to a slowdown of the equilibration rate due to decreased permeability of the membrane. Regular cleaning can minimize the effect of biofouling, but additional biofouling protection aide in providing accurate measurements for a longer period of time.

Since the quality of the measurement is involved, the fouling protection, especially on the sensitive part of the sensor, must be effective. By reducing fouling, operational lifetime of the instrument is extended. This results in a more cost-effective instrument due to less maintenance required. The ideal protection should be of low cost, require low power, be easy to install on existing sensors, and require low maintenance. Furthermore, there should be no adverse effects on the measurements and no modification of the local environment to be monitored. Over the years, numerous attempts to minimize the effects of fouling on structures exposed to an aquatic environment have been done. The techniques can be classified into various categories, including mechanical (e.g., wiper, brush, water jet, and ultrasonic sound) and biocidal (e.g., copper, chlorine, and UV) approaches. (Yoon et al., 2016). While some methods show interesting results in the laboratory, the real in situ tests can be very disappointing due to the complexity of the in situ environment. (Shukla et al., 2017)

Today, the three most common antifouling protections systems are purely mechanical devices such as wipers, uncontrolled biocide generation systems based on copper corrosion mechanism, and controlled biocide generation systems based on localized seawater electro-chlorination systems or automatic acid dispensing devices. Cleaning methods involving high pressure jets or brushes may modify the status of the sensitive sensor area. Surface treatment based on antifouling paints (biocide release coatings or self polishing coating) are useful antifouling mechanisms. However, certain biocidal coatings have been linked to environmental problem such as tributyltin. Copper is known for its biocide properties due to the release of bivalent Cu^{2+} which interferes with enzymes on cell membranes and prevents cell division. This exhibits antifouling activity against organisms such as barnacles, tube worms and the majority of algal fouling species. Compared with other biocides, the relatively low toxicity of copper ensures effective application in aquatic en-

vironmental monitoring. (Voulvoulis et al., 1999) Protection based on a dissolving biocide such as chlorine or bromine tablets have been used in closed systems, but there are difficulties in delivering a steady and uniform concentration during deployment. Techniques based on irradiation which do not generate any biocide is promising, although they require power. (Delauney et al., 2010)

2.4.1 Membrane technology

Fouling of membranes results in a decreased membrane life. Thus, a large part of research in membrane technology is focused on the development of antifouling membranes and several techniques have been employed. This include surface modification by coating, rafting and the concept of making thin film composites (TFC) membranes, bulk modification by blending and mixing polymers, and incorporation of nanomaterials into membrane matrices to develop nanocomposite membranes. Recently, the study of nanocomposite membranes has grown as an active area of membrane materials research and development. The nanomaterials of greatest interest for nanocomposite membrane development are metal oxide nanoparticles with antimicrobial activity such as titanium oxide (TiO_2), aluminum oixide (Al_2O_3), zinc oxide (ZnO), silicon dioxide (SiO_2), and graphene oxide (GO). Among them, GO is an emerging nanomaterial that has shown great promise in the development of antifouling nanocomposite membranes. The additional advantage of using GO as nanoadditive is that is can be processed easily owing to the availability of functional groups such as hydroxyl, carbonyl and carboxyl located on its surface and edge, which help to disperse it into the membrane matrix. Apart from these, its antibacterial properties, low toxicity, chemical and biological durability and low cost make GO a promising nanomaterial for the development of antifouling nanocomposite membranes. (Shukla et al., 2017)

Polydimethylsiloxane (PDMS) is one of the most important high performance polymers and can be used in many conventional technologies, such as adhesive, sealing and coating but it also has great potential for applications in biomaterial science because of its chemical inertness, thermal stability and bio-compatibility. ZnO exhibits selective toxicity to bacteria and show low toxic effect on human cells, permitting their use in agricultural and food industries. On modification of ZnO nanoparticles in PDMS the transformation from hydrophobic to superhydrophobic surface can be achieved. (Wu et al., 2005) In a 45 day sea trial, ZnO nanocomposite incorporated in PDMS performed with 80 $\%$ reduction of macrofouling compared to the control. Metal leaching from the nanocomposites were found to be about 1000 times less than from conventional antifouling coatings, indicating minimal environmental effect. (Sankar et al., 2015)

2.5 Inductively Coupled Plasma Mass Spectrometry (ICP-MS)

Inductively Coupled Plasma Mass Spectrometry (ICP-MS) has grown to be one of the most important techniques for elemental analysis since the 1980s. The technique presents low detection limits for most elements, a high degree of selectivity and a reasonable good precision and accuracy. Sample solutions are normally introduced into the instrument by a nebulizer, and an ICP torch serves as an atomizer and ionizer. Positive metal ions, produced by the ICP torch, are sampled through a deferentially pumped interface linked to a mass analyzer, usually a quadrupole, and dispersed in the mass analyzer based on their mass-to-charge ratio (m/z). The produced spectra consists of series of isotope peaks for each element present, and are used to identify the elements present in the sample and quantify them. Usually, quantitative analyzes are based on calibration curves.

The quadropole mass analyzer is more compact, less expensive, more rugged, and presents higher scan rates than other spectrometers. It consists of four parallel cylindrical rods that serve as electrodes. Opposite rods are connected electrically, one pair attached to the positive side of a variable dc source, and the other pair attached to the negative terminal. Variable radio-frequency ac voltages are applied to each pair of rods. Mass spectra are obtained by ions accelerating into the space between the rods by a potential difference of 5 to 10 V. Meanwhile, ac and dc voltages on the rods are increased simultaneously while maintaining their ratio constant. At a given moment, all of the ions except those having a limited range of m/z values reach the transducer. (Skoog, 2007)

The interference's related with this technique include spectral overlaps generated by combinations of argon, solvent, and/or ionic species from the sample, and physical suppression of the analyte signal brought on by the level of dissolved solids or acid in the sample among others. Modern instrumentation and good software combined with optimized analytical methodologies minimize the negative impact of these interference's. (Thomas, 2004)

2.6 Statistics

Statistics are used to evaluate the quality of experimental measurements, test hypotheses, and develop models to describe experimental results. The variance, s^2, is a measure of spread in the data set and can be calculated as shown in Equation (2.32). x_i is the value for sample number i, $\bar{x}$ is the sample mean and N is the total amount of sample values. The equation for calculating the mean, $\bar{x}$ can be seen in Equation (2.33). The standard deviation, s, is the square root of the variance, s^2. (Walpole et al., 2012)

$$s^2 = \frac{\sum_{i=1}^{n}(x_i - \bar{x})^2}{N-1} \tag{2.32}$$

$$\bar{x} = \frac{\sum_{i=1}^{n} x_i}{N} \tag{2.33}$$

2.6.1 One-Sample T-Test

The One-Sample T-Test is used to determine whether a sample comes from a population with a specific mean. The procedure includes stating the null hypothesis, H_0: $\mu = \mu_0$ and forming the test statistics, t. μ_0 is a specific value of μ such as an accepted value, a theoretical value or a threshold value.

$$t = \frac{\bar{x} - \mu_0}{s/\sqrt{N}} \tag{2.34}$$

Further, the alternative hypothesis, H_a and rejection region must be stated. The critical value of t, t_{crit}, is a point on the test distribution that is compared to the test statistic to determine whether to reject the null hypothesis.
For H_a: $\mu \neq \mu_0$, reject H_0 if t $\geq t_{crit}$ or if t $\leq$ - t_{crit} (two-tailed test)
For H_a: $\mu > \mu_0$, reject H_0 if t $\geq t_{crit}$ (one-tailed test)
For H_a: $\mu < \mu_0$, reject H_0 if t $\leq$ - t_{crit} (one-tailed test)

The assumptions of this test include that the dependent variable are continuous (such as time), the data are independent, no significant outlayers, and that the dependent variable should be approximately normally distributed. (SPSS, 2018c)

2.6.2 Normality tests

Normality tests can be performed to assess the normality of the data, such as the Shapiro-Wilk Test and Normal Q-Q-Plot. If the significant value of the Shapiro-Wilk Test is greater than 0.05, the data is normal. If it is below 0.05, the data significantly deviate from a normal distribution. In a Normal Q-Q Plot, the data are normally distributed if the data points are close to the diagonal line while the data are not normally distributed if the data points deviate from the line in an non-linear fashion. (SPSS, 2018d)

2.6.3 Friedman and Kruskal Wallis H test

Friedman test is used to compare distributions of several related variables, and is the non-parametric alternative to the one-way analysis of variance (ANOVA) with repeated measures. Non-parametric tests do not assume the data follow a normal distribution. Friedman tests the null hypothesis that k related variables come from the same population. For each case, the k-variables are ranked from 1 to k. The test statistics are based on these ranks. The Friedman test assumes one group that is measured on three or more different occasions, a group is a random sample from the population and that the dependent variable should be measured at ordinal or continuous level, for example time measured in hours. (SPSS, 2018a)

The Kruskal-Wallis H test is the nonparametric analog of one-way ANOVA and is a method for determining if there are statistically significant differences between two or more groups of an independent variables on a continuous or ordinal dependent variable. The test assumes independence of observations, which means that there is no relationship between the observations in each group or between the groups, and that the group distributions have the same shape. (SPSS, 2018b)

2.6.4 Visualization of data

Curve fitting is often used for data visualization, and construct a curve or a mathematical function that has the best fit to a data set. Curve fitting can involve interpolation, where an exact fit to the data is required, or smoothing, where a smoothing function approximately fits the data. The smoothing function, yy, of a data set y, can be a moving average filter where the first few elements of the function are given under. (TheMathWorks, 2014a)

yy(1) = y(1)
yy(2) = (y(1) + y(2) + y(3))/3
yy(4) = (y(1) + y(2) + y(3) + y(4))/5
yy(5) = (y(2) + y(3) + y(4) + y(5))/5
...

Most commonly, coefficients of a polynomial, p(x), of degree n are found to fit a data set. The polyfit Matlab function finds the coefficients of a polynomial, p(x), of degree n that fits the data, y, by minimizing the sum of the squares of the deviations of the data from the model (least-squares fit). The function forms the Vandermonde matrix V, whose elements are powers of x and uses the backslash operation to solve the least squares problem. The output of the function is the polynomial coefficients in descending power and an error estimation structure containing the norm of the residuals among other things. The Matlab function polyval evaluates the polynomial p at each point in x, and can be used to plot the polynomial.

To validate the model, the original data and the model can be plotted in the same plot. In addition, the maximum of the absolute value of the deviation of the data from the model can be found. A value much smaller than any of the data values indicate a model which accurately follows the data. (TheMathWorks, 2014b)

$$\mathrm{MaxErr} = max(abs(yy - y)) \tag{2.35}$$

Chapter 3

Experimental

3.1 Pro-Oceanus Solu-Blu dissolved carbon dioxide sensor

Measurements with Pro-Oceanus Solu-Blu dissolved carbon dioxide (CO_2) sensor were performed both at Nofima, Sunndalsøra and at the Norwegian University of Science and Technology (NTNU), Trondheim. The standard product includes the sensor with the open faced head, Teflon membrane and 3 meters of cable (Figure 3.1). In the laboratory at NTNU, the sensor was connected to a computer to provide live monitoring while it was connected to a logging cabinet where the output were stored on a memory stick at Nofima.

Figure 3.1: Pro-Oceanus Solu-Blu dissolved carbon dioxide (CO_2) sensor with the open faced head and Teflon membrane.

Physical sensor specifications are presented in Table 3.1.

Table 3.1: Physical Pro-Ocenanus Solu-Blu sensor specifications.

Parameter	**Specification**
Length	20 cm 26 cm with connector
Diameter	5 cm
Weight	0.28 kg
Housing material	Acetal plastic
Depth rating	0 - 50 meters
Water temperature range	-2 to 40 °C

Sensor calibration was performed by staff at Pro-Oceanus Systems Inc. December 2018. Sensor performance specifications are given in Table 3.2.

Table 3.2: Pro-Ocenanus Solu-Blu sensor performance specifications.

Parameter	**Specification**
Measuring principle	NDIR (Non-Dispersive Infrared)
CO_2 measurement range	0-50 mg/L
Accuracy	CO_2: $\pm$ 2% (of maximum range) TDGP: $\pm$ 0.1 % (0-2 bar range) Temperature: $\pm$ 0.5 °C
Equilibration rate (t_{63})	pCO_2: 4 minutes TDGP: 10 minutes
Sensor warm up time	3 minutes
Resolution pCO_2	0.1 % of max range

3.1.1 Experiments with the Solu-Blu sensor

The experiment using the Solu-Blu dissolved carbon dioxide (CO_2) sensor was divided into four parts, where one antifouling mechanism was tested in each part. The four mechanisms to minimize biofouling are shown in Figure 3.2. These mechanisms were a polytetrafluoroethene (PTFE or Teflon) membrane (a), a copper grid (b), a polydimethylsiloxane (PDMS) membrane (c), and a water-pumped flow-through head (d). The Teflon membrane and water-pumped flow-through head were produced by Pro-Oceanus Inc. The copper grid was ordered at the mechanical workshop at NTNU with a diameter to fit the open faced head and a grid size at 5 mm. Graphene oxide (GO) and zinc oxide (ZnO) was incorporated as nanoadditives into polydimethylsiloxane (PDMS) to develop a PDMS/GO-ZnO nanocomposite membrane with enhanced antifouling properties by a PhD student at NTNU. This membrane had a variable thickness, variating from 2 to 1 mm. As the PDMS/GO-ZnO nanocomposite membrane was not previously tested for water resistance,

it was tested together with the Teflon membrane to ensure that no water infiltrated the detector during measurements and resulted in a layer of air between the two membranes. A preliminary absorption test of the PDMS based membrane was conducted by placing a piece of the PDMS based membrane in water for two weeks and weighing it before and after. In all experiments, except for the part with the water-pumped flow-through head, the open faced head was used.

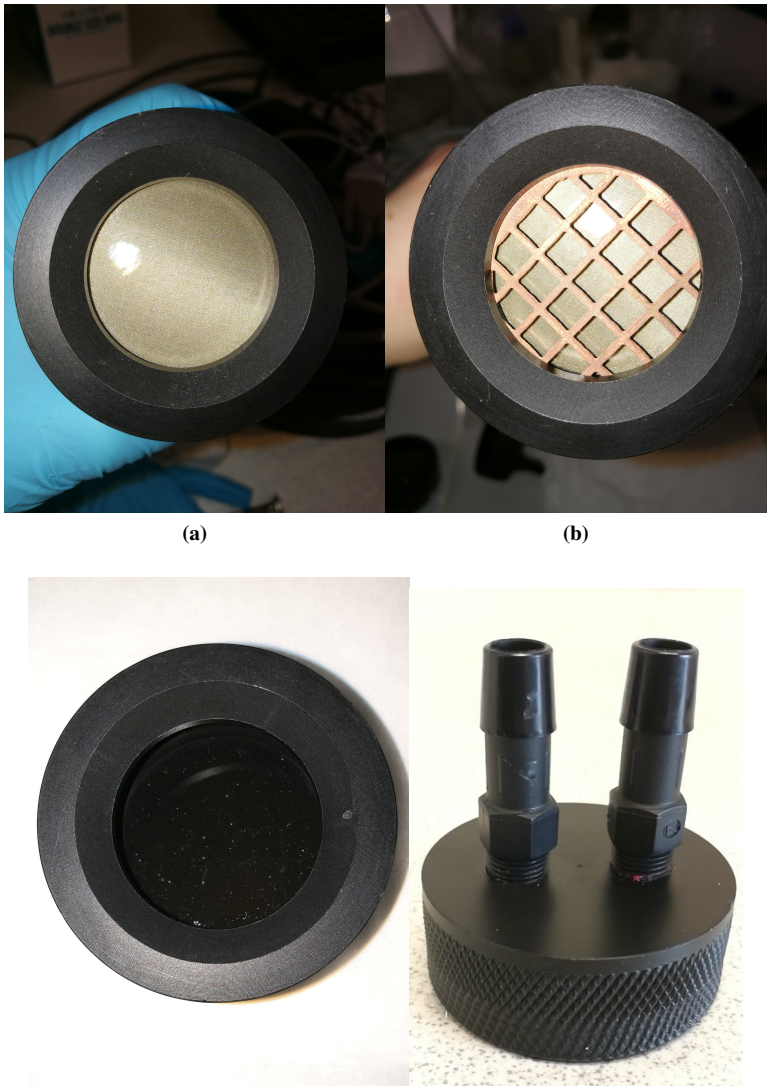

(a) **(b)**

(c) **(d)**

Figure 3.2: Open faced head with (a) Teflon membrane, (b) Teflon membrane and copper grid and (c) PDMS membrane. (d) Water-pumped flow-through head.

3.1.2 Installing an antifouling mechanism

When a new antifouling mechanism was applied, the faceplate of the sensor had to be removed. Before unscrewing the faceplate, the housing of the sensor was dried. The sensor was placed horizontally on a dry surface of several dust-free tissues before the faceplate was unscrewed to prevent water to enter the sensor. After the faceplate was unscrewed, water from the threads of the head was dried with dust-free tissues and the membrane support area was inspected for any water. The membrane was examined for scratches and every surface was dabbed dry using dust-free tissues before the membrane was placed back onto the membrane support with the shiny side facing outwards. The two o-rings were greased with G-9030 silicone grease from NuSil Technology and put in their respective place before the faceplate was screwed on and tightened. In the case of the water-pumped flow-through head, this head was screwed on instead of the open faced head as seen in Figure 3.3. During this process, the copper grid or PDMS membrane were placed between the o-ring over the Teflon membrane and the faceplate.

Figure 3.3: Installing the water-pumped flow head. (Pro-Oceanus, 2018)

After a new antifouling mechanism was installed, the output data was monitored for one hour to ensure that the sensor gave reasonable output values, and in the case of the pumped head, the sensor was tested in fresh water for one hour while monitoring the data to ensure no leakage of water behind the membrane.

3.1.3 Laboratory tests

The Solu-Blu sensor with all four antifouling mechanisms were tested in laboratory conditions before measuring at Nofima. In the laboratory, the sensor was directly connected to a computer through a deck box delivered by Pro-Oceanus Systems Inc. as seen in Figure 3.4. Tera Term was used as terminal program. The laboratory experiments were performed in tap water and tap water spiked with CO_2, thus the salinity input in Tera Term was set to 0 ppt. The baud rate was set to 19200. CO_2 spiked water was made by exhaling through a straw and into the solution for approximately 3 minutes.

Figure 3.4: Instrument setup with the deck box from Pro-Oceanus. (Pro-Oceanus, 2018)

The experimental setup for tests using the open faced head in the laboratory is presented in Figure 3.5. Stirring with a magnetic stirrer was used on level 4 out of 10 when the open faced head was used. Once the sensor was immersed into the water, it was tilted to a horizontal position to ensure that gas was not trapped on the membrane interface before it was tilted back to vertical position. The sensor was gently rinsed with tap water before it was placed in a new solution.

The sensor measured 20 minutes in tap water, 20 minutes in CO_2 spiked water and 20 minutes in tap water in all laboratory tests, except when testing the PDMS membrane. In this test, the sensor measured 20 minutes in tap water, 1 hour in CO_2 spiked water and 2 hours in CO_2 free water.

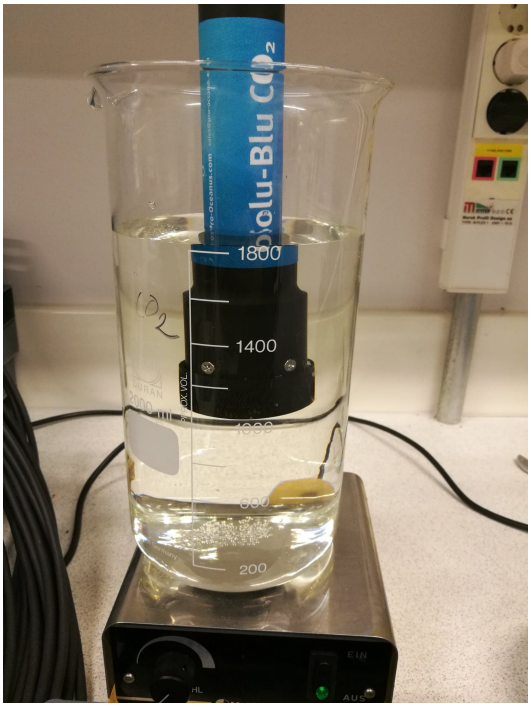

Figure 3.5: Experimental setup in the laboratory for measuring with the Pro-Ocenanus Solu-Blu CO_2 sensor.

In addition to testing all the antifouling mechanisms, the impact of an air bubble accumulated on the membrane interface and how the concentration of CO_2 in a CO_2 spiked solution changed over time were tested. Two identical tests in the same solutions were performed to assess the impact of an air bubble accumulated on the membrane interface. An air bubble covering 1/5 of the membrane interface was present in the first test and removed before the second test. The change in CO_2 concentration for a spiked CO_2 solution were tested by analyzing in a CO_2 spiked solution over a period of four hours.

For the experiment with the water-pumped flow-through head, Eheim CompactOn 300 aquarium pump was placed in a water supply beaker and connected to a hose which transported water to the pumped head. This setup can be seen in Figure 3.6. Another hose transported water from the pumped head and back to the water supply container. The flow rate in the hose was adjusted with a valve to 0.3 L/min. When the solutions were changed, the supply container was emptied as much as possible, but still contained enough water such that the pump was always under water. This was done to prevent air flowing through the hose. When the supply container was emptied to the minimum, the new solution was poured carefully into the container. Even though this was done carefully, the water flow may have been slightly changed. The test was performed 10 minutes in tap water, 20 minutes in spiked CO_2 water, and 20 minutes in tap water. The CO_2 spiked solutions in these experiments were not the same due to the different experimental set ups, but it was tried to exhale the same amount of air into both solutions.

(a)

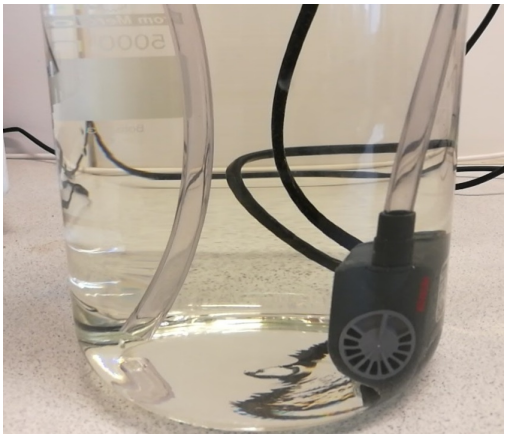

(b)

Figure 3.6: (a) The water-pumped flow-through head installed on the sensor. (b) Eheim CompactOn 300 aquarium pump providing water to the water-pumped flow head from a water supply beaker.

3.1.4 Measurements at Nofima, Sunndalsøra

At Nofima, the Solu-Blu sensor measured continuously for two weeks in water from Recycling Aquaculture System (RAS) tank 1 in Veksthall 1 (VH1). The tank contained 723 salmon broodfish with average weight 10.8 kg. The fish were fed with approximately 25 kg feed each day evenly distributed from 08:00 to 22:00 by an automatic disc feeder. The photoperiod started at 08:00 each day, and decreased from 15 to 13 hours during the weeks

of measurements. The tank volume and water flow were 100 m^3 and 2500 L/min respectively. To provide a qualitative estimate of biofouling during the experiment at Nofima, photographs were taken of the experimental setup.

The sensor was connected to a logging cabinet delivered by Christian Berner AS at Nofima. The output data were saved as Comma Separated Variables (CSV) on an USB stick placed inside of the logging cabinet. The logging cabinet (a) and hinges to attach the cabinet (b) can be seen in Figure 3.7.

(a)

(b)

Figure 3.7: The logging cabinet from Christian Berner AS (a) and hinges to attach the cabinet (b).

Positive values of slope and interception of regression curves for partial pressure of CO_2 (pCO_2) and Total Dissolved Gas Pressure (TDGP) were selected on the touch screen in the front of the logging cabinet. These values were given by Pro-Oceanus and can be seen in Table 3.3 together with input values for logging interval, temperature, O_2 saturation and salinity. The temperature, O_2 saturation and salinity were set as the average values of the water in the studied tank.

Table 3.3: Input values for temperature, O_2 saturation, salinity, air pressure and logging interval used at Nofima. Regression curves for Total Dissolved Gas Pressure (TDGP) and partial pressure of CO_2 (pCO_2).

Parameter	**Value**	
Temperature [°C]	12	
O_2 saturation [%]	89	
Salinity [ppt]	13	
Air pressure [mBar]	1000	
Logging interval [s]	300	
TDGP regression curve	y = 31.969x + 670.84 y= 100x + 799	(mA output) (V output)
pCO_2 regression curve	y=3.201x - 12.9 y=10.02x - 0.2004	(mA output) (V output)

Three of the four parts of the experiment at Nofima were conducted in a by-pass. The by-pass was set up by letting water flow through a water hose from the side wall drain of the tank and into a plastic bucket. The water flowed through the hose with the help of gravity, and the water flow was set to 3 L/min with the help of a valve. The sensor was immersed into the bucket, and measured continuously for two weeks. The housing of the sensor was covered with duct tape to make it easier to clean. Figure 3.8 shows the by-pass (a) and the valve controlling the water flow (b). A plastic object was immersed into the by-pass to compare the amount of fouling on this object and the sensor when measuring with the copper grid and the PDMS membrane.

For the part with the water-pumped flow-through head, the water flow was controlled with a valve and set to 1.5 L/min. The set up was tested in fresh water for about one hour while monitoring the output data to ensure no leakage of water behind the membrane.

(a)

(b)

Figure 3.8: (a) The by-pass setup. (b) The valve controlling the water flow.

3.1.5 Washing procedure

After the experiments, the duct tape was removed from the sensor housing and the membrane was cleaned to ensure fast response time and prolonged service life. A small bucket filled with clean fresh water was used at the laboratory, while Deconex 11 diluted in clean fresh water was used at Nofima for cleaning. The sensor was placed in the bucked with a small water circulation (less than 3 L/min) provided by Eheim CompactON 300 aquarium pump until the membrane was clean when using the open faced head. In the case of the pumped head, the aquarium pump was used in the same way, but to flush water through the hose that transfers water to the sensor head at 1.5 L/min for 30 minutes.

3.1.6 Water behind the membrane

When water was observed under the membrane of the sensor after measuring at Nofima, the sensor was detached from the logging cabinet and brought to NTNU for drying. The sensor was dried for 24 hours in a closed container with silica gel where it was made sure that no particles entered the sensor. During drying, the membrane and o-rings were removed.

After the drying, the sensor was tested in the laboratory to see if it responded normally. The test was performed by measuring 20 minutes in tap water, 20 minutes in CO_2 spiked tap water and then 30 minutes in tap water. If the sensor did not respond to changes in CO_2 concentration, the sensor was opened to look for damages in the electronics and if no damages could be seen, additionally drying were performed until the sensor responded normally to changes in CO_2 concentration.

3.2 Franatech hanheld carbon dioxide sensor

Measurements of carbon dioxide (CO_2) with Franatech hanheld CO_2 probe were conducted once a week during the experiment by staff at Nofima. This was done by inserting the probe in the side wall drain, waiting 20 minutes, turning it on, and then reading the measurements 20 minutes after. Figure 3.9 shows the probe in the side wall drain of tank 1 in VH1. The output values were given in vpm and together with the temperature, the concentration of CO_2 were calculated.

Figure 3.9: The Franatech handheld sensor measuring in the side wall drain of tank 1 in Veksthall 1 at Nofima.

3.3 Total Inorganic Carbon (TIC)

Total Inorganic Carbon (TIC) measurements were conducted once a week by staff at Nofima. The samples were collected in clean glass bottles rinsed three times with the sample solution before collecting the sample. The flasks were filled completely to the top so no air was inside the flasks and put on ice before transferring it to the laboratory for analysis. In the laboratory, TIC was analyzed using Flow Solution IV, Autosampler Model 3360 and Expanded Range (ER) photometric detector delivered by O-I-Analytical. The instrument was calibrated with dried sodium carbonate solutions of 2, 4, 5, 10, 30 and 60 mg/L.

The pH and temperature were measured with Hach HQ40D Portable Multi Meter and the salinity was measured with a handheld refractometer with automatic temperature compensation from VWR. The concentration of CO_2 were calculated from TIC, pH, salinity and experimentally determined dissociation constants.

During one day, TIC samples were collected by the master student at 08:00, 10:00, 12:00, 14:00 and 16:00. In addition, pH, temperature and salinity were measured. These TIC samples were analyzed the next day at the Nofima laboratory, but the three first samples were additionally analyzed right after collection. The samples were stored in the refrigerator when not used.

3.4 Classical titration with sodium hydroxide

Classical titration with sodium hydroxide (NaOH) were performed in the beginning and end of each part of the experiment, except for in the beginning of the first part. Discrete water samples from the RAS tank were completely filled in clean plastic bottles with a tight-fitting cap to minimize gas exchange with the atmosphere. The bottles were rinsed three times with the sample solution before collecting the sample.

The buret was filled with titrant, and 200 mL of sample was poured into a Erlenmeyer flask in 3 parallels. 4 drops of phenolphtalein indicator was added to the sample and swirled. If a pink color was observed, no carbon dioxide was in the sample. If no pink color was observed, titrant was added to the sample under swirling until a light pink color appeared for a minimum of 30 seconds. The concentration of carbon dioxide in mg/L CO_2 in the sample was calculated. The samples were analyzed within two hours after collection.

3.4.1 Sodium hydroxide standard solution

CO_2 free water was made by boiling MilliQ Ultrapure water for 10 minutes and store it in a closed container with Ascarite to adsorb CO_2. A sodium hydroxide (NaOH) solution was prepared by weighing out about 4.5 g NaOH beads and transferring them to a 400 mL beaker. The beads were rinsed with a small amount of CO_2 free water to remove Na_2CO_3 present on the bead surface. About 150 mL CO_2 free water was added to the beaker, and the solution was stirred with a glass rod to prevent beads to aggregate themselves. CO_2 free water was slowly added until a total volume of about 300 mL was reached. When all material was dissolved, the solution was transferred to a 1 L plastic bottle and CO_2 free water was added to a total volume of about 1000 mL. The bottle was tightly capped, and mixed well.

3.4.2 Standardization of the sodium hydroxide solution

Potassium hydrogen phthalate (KHP) was predried at 110 degrees for 2 hours and put in a desiccator for storage. 3 individual samples of about 0.2 g potassium hydrogen phtalate were weighed out in 3 250 mL Erlenmeyer flasks, and added about 50 mL of pure water. 2 drops of phenolphtalein indicator was added, and the samples were titrated against the NaOH solution until the pink color of the indicator persisted for about 30 seconds. CO_2 free water was titrated as a reference sample. The concentration of the NaOH solution was determined. The standardization of the sodium hydroxide solution was performed one day before or after each titration of water samples.

3.5 ICP-MS analysis

Discrete water samples from the tank were collected in clean plastic bottles rinsed three times with the sample solution. The samples were filtrated with Whatman 1820-055 Grade GF/A Glass Fiber Filter Paper and poured into clean 15 ml polyethylene tubes. The tubes were acidified with 1 droplet of Ultra pure 65% nitric acid (concentrated) from VWR per 3.3 mL sample. 8800 Triple Quadrupole Inductively Coupled Plasma Mass Spectrometry (ICP-MS) was used to analyze the samples, and done by staff at the Norwegian University of Science and Technology (NTNU). This was only a minor part of the experiment.

3.6 Statistics

3.6.1 SPSS Statistics

In SPSS Statistics, normality tests were performed to assess normality. These tests were done by clicking Analyze, Descriptive statistics and Explore. Further, Statistics were clicked and Descriptives with confidence interval for mean 95 % were chosen. Descriptive Histogram, Boxplot with factor levels and Normality plots were chosen in Plots.

One-Sample T-Tests were performed to compare the mean of 13 Solu-Blu measurements with the calculated CO_2 values. The selected 13 Solu-Blu measurements were the sensor readings in an interval of one hour from the time the samples to calculate CO_2 were collected. If the samples to calculate CO_2 were collected at 10:00, measurements with the Solu-Blu sensor from 09:30 to 10:30 were used to calculate the mean. The test was performed by clicking Analyze, Compare Means and One-Sample T Test. Further, sensor measurements were selected in Test Variables, while the calculated CO_2 value was inserted in Test Value.

A Friedman test with pairwise comparisons were performed of the data set from the experiment with the open faced head. This was to test if sample distributions of the different days of the data set came from the same population with significance level 0.05. The data set were divided into groups of 24 hours of sampling. The Friedman test was done by clicking Analyze, Nonparametric tests and Related samples. Customize analysis were chosen in objective, and the CO_2 measurements were selected for the Test field in Fields while group number were maintained in Fields. Customize tests and Friedman's 2-way ANOVA by ranks (k samples) were selected in Settings.

To see if the distributions of CO_2 concentration were the same for day 3 to 6 for the four parts of the experiment at Nofima with significance level 0.05, a Kruskal-Wallis H test was performed. 880 measurements were in each group. The test was performed by clicking Analyze, Nonparametric Tests, Legacy Dialogs and K Independent Samples. Further, CO_2 concentrations were selected in the Test Variable List and the groups were selected in the Grouping Variable. Minimum and Maximum were selected to be 1 and 4 respectively in the Define Range box. Options was clicked, and Descriptice and Exclude cases test-by-test were chosen.

3.6.2 MatLab

The data sets were plotted with error bars of one standard deviation of uncertainty. A smoothing function with a moving average filter were used when comparing daily variations for the 4 different parts of the experiment.

For polynomial curve fitting of the data sets, the function polyfit in Matlab found the coefficients of a polynomial of degree 2 that fitted the data set in a least square sense. Polyval returned the value of the polynomial evaluated at x, and were used to plot the results. The polynomials were evaluated by plotting them together with the original data. The maximum error between the model and data sets were found.

Chapter 4

Results and Discussion

4.1 Laboratory testing

Before the two week measurement in Recycling Aquaculture Systems (RAS) at Nofima, the Pro-Oceanus Solu-Blu dissolved carbon dioxide (CO_2) sensor was tested in laboratory conditions with all four mechanisms to minimize fouling. This was done to see how the antifouling mechanisms affected the sensor readings. Further, it was made sure that the instrumental setup worked properly in fresh water before measuring in water with higher salinity. When the membrane type is not specified, the Teflon membrane was used. The Pro-Oceanus Solu-Blu CO_2 sensor will be referred to as the sensor in this and later sections. Enlarged versions of all graphs presented in this section can be found in Appendix for a closer examination.

4.1.1 Water-pumped flow-through head

The response time of the water-pumped flow-through head was compared to the response time of the open face head in laboratory conditions (10 minutes in tap water, 20 minutes in CO_2 spiked water and 20 minutes in tap water). The results are shown in Figure 4.1 (Enlarged: Figure A.1 in Appendix). When using the open faced head, the sensor readings showed approximately 0 mg/L CO_2 when measuring in tap water. Further, the readings increased when it was transferred to the CO_2 spiked water. Lastly, the readings decreased when the sensor was moved back to tap water.

When using the pumped head, sensor readings increased more rapidly when the solution was changed from tap water to CO_2 spiked water. After some minutes, the readings decreased before a stable concentration was achieved at approximately 10 mg/L CO_2. A possible reason for this decrease was that when the solution in the water supply beaker was changed from tap water to CO_2 spiked water, there was tap water in the outlet hose which decreased the CO_2 concentration in the supply beaker when it was mixed. From this result, it can be seen that the pumped head provide faster response time than the open faced head.

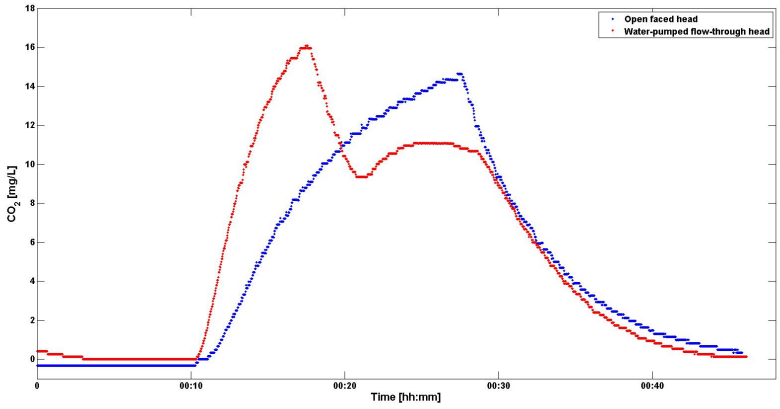

Figure 4.1: Sensor readings when testing the pumped head and open faced head in the laboratory. The experiments were performed 10 minutes in tap water, 20 minutes in CO_2 spiked water, and 20 minutes in tap water.

4.1.2 Copper grid

Sensor readings with and without the copper grid were compared in the laboratory, and the results are presented in Figure 4.2 (Enlarged: Figure A.2 in Appendix). The two tests were performed in the same solutions, 10 minutes in tap water, 20 minutes in CO_2 spiked water, and then 20 minutes in tap water.

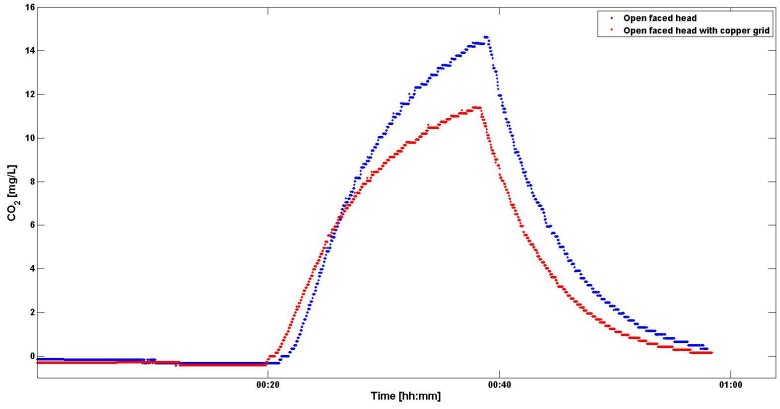

Figure 4.2: Sensor readings when testing the sensor with and without the copper grid in the laboratory. The tests were performed 10 minutes in tap water, 20 minutes in CO_2 spiked water, and then 20 minutes in tap water.

The test without the copper grid was performed two hours before the experiment with the copper grid. From the figure, it can be seen that the peak when using the copper grid was lower than the peak when not using the copper grid. In a CO_2 spiked solution, the concentration of CO_2 decreases with time. This is visualized in Figure 4.3, where the sensor measured 20 minutes in tap water, and then over 3 hours in CO_2 spiked water (Enlarged: Figure A.3 in Appendix). This may be the reason why the peak with the copper grid was lower than without the copper grid. From these results, it may seem like the copper grid do not affect the response time or accuracy of the sensor.

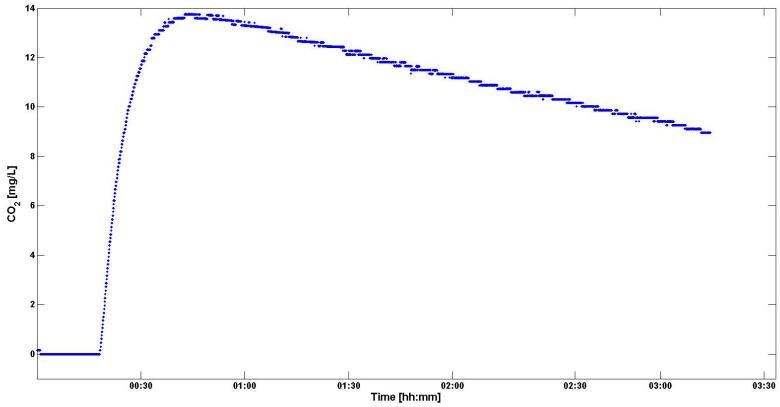

Figure 4.3: The concentration change of a spiked CO_2 solution over time. The experiment was performed 20 minutes in tap water and then over 3 hours in CO_2 spiked water.

4.1.3 Polydimethylsiloxane (PDMS) membrane

Response times when using the Teflon membrane together with the polydimethylsiloxane (PDMS) membrane and the Teflon membrane alone are presented in Figure 4.4 (Enlarged: Figure A.4 in Appendix). The PDMS membrane was placed over the Teflon membrane and its associated o-ring which resulted in a layer of air between the two membranes. This was done to ensure that no water entered the sensor due to that the PDMS membrane had not yet been tested for water resistance, and a prolonged response time was expected for this set-up. However, a small piece of the PDMS based membrane was placed in water for two weeks to see how it behaved. After two weeks, the piece had gained 0.0031 g which corresponds to a 0.6 % weight increase. Calculations are shown in Table A.1 in Appendix. The weight gain may be due to not drying the membrane completely before weighing.

These two tests were not performed in the same solutions, but it was tried to exhale the same amount in both test solutions. This may have resulted in the CO_2 spiked solution had a different concentration of CO_2, but the response time when using the PDMS membrane is still undoubtedly slower. During the experiment, small air bubbles was observed on the PDMS membrane which also may have contributed to the prolonged response time.

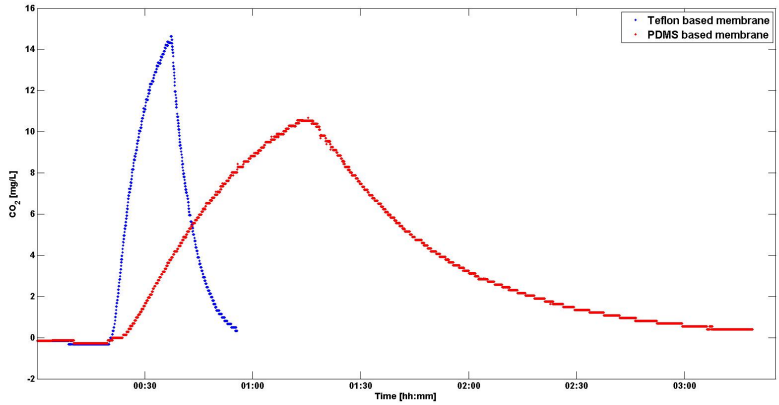

Figure 4.4: Response times for the Teflon membrane and the polydimethylsiloxane (PDMS) membrane together with the Teflon membrane in laboratory conditions. After 20 minutes in tap water, the sensor was moved to a CO_2 spiked solution in both experiments. For the Teflon membrane, the experiment was performed 20 minutes in the CO_2 spiked solution before it was moved back to tap water, while the PDMS membrane was tested in 1 hour in CO_2 spiked water before it was moved back to tap water.

4.1.4 Air bubble accumulated on the membrane interface

Two tests were conducted to explore how an air bubble accumulated on the membrane interface affected the readings of the sensor. The experiments were performed 10 minutes in tap water, 20 minutes in CO_2 spiked water, and lastly 20 minutes in tap water. First, a test with an air bubble accumulated on the membrane surface was conducted. Thereafter, the air bubble was removed and the same experiment was performed in the same solutions. The result can be seen in Figure 4.5 (Enlarged: Figure A.5 in Appendix). As mentioned before, the concentration in a CO_2 spiked solution decreases with time. As the experiment with the air bubble on the membrane interface was conducted first, it was expected that the concentration in this solution would be a bit higher than in the second experiment if the air bubble did not have an effect on the sensor reading. As the opposite was observed, it can be concluded that accumulation of air bubbles on the membrane surface results in a slower response time and reduces the accuracy of the sensor.

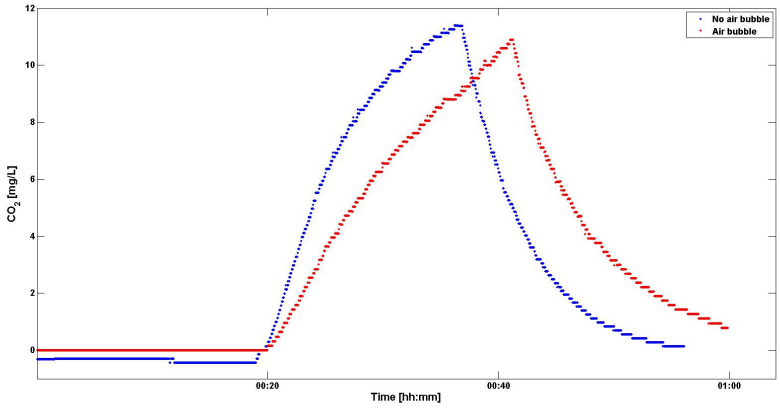

Figure 4.5: Sensor readings using the open faced head with and without an air bubble accumulated on the membrane interface. The experiments were performed 10 minutes in tap water, 20 minutes in a spiked CO_2 solution, and lastly 20 minutes in tap water.

4.2 Measurements at Nofima

In the following subsections, the results from testing of the Pro-Oceanus Solu-Blu CO_2 sensor at Nofima will be presented and discussed. Enlarged versions of all graphs presented in this section can be found in Appendix for a closer examination. Measurements from the Solu-Blu sensor are not included in Appendix, but can be obtained upon request. The Solu-Blu sensor was not installed directly into the aquaculture system. This was due to a high water flow in the side-wall drain, and the possibility of air bubbles accumulating on the sensor membrane due to fish activity in the fish tank. Further, biocidal material was used in the experiment which may leach into the water. Considering this, the sensor was put in a secondary connection to where the water was not transferred back into the recirculating system.

Measurements with the open faced head and water-pumped flow-through head were tested first to evaluate how the two next experiments should be set up. Pumping of liquid directly onto the membrane would help reduce the amount of biofilm forming on the membrane interface, and it was therefore considered to combine the pumped head with the copper grid and PDMS membrane if the experiment with the pumped head was successful. Due to water penetrated behind the sensor membrane when using this head, the combination of the pumped head with other antifouling mechanisms were not used in the two last parts of the experiment but set up in the same way as the experiment with the open faced head. This will be further discussed in a later subsection. The water flow into the by-pass and pumped head were selected to be high enough to reduce fouling of the membrane, but low enough to not damage the membrane. Therefore, 3 L/min of water was used as the inlet water flow in the by-pass. On the other hand, a flow of 1.5 L/min was used with the pumped head as water flow of 1-3 L/min was recommended by the producer.

4.2.1 Reference measurements

At Nofima, reference CO_2 measurements were made by calculating the CO_2 concentration from Total Inorganic Carbon (TIC), pH, salinity (S), temperature (T) and experimentally determined dissociation constants. In addition to this, reference measurements with Franatech handheld CO_2 sensor were conducted. The results from these measurements are presented in Table 4.1. Additional information used to calculate the Franatech measurements are shown in Table B.1 in Appendix.

Table 4.1: Results from Franatech measurements, $CO_{2Franatech}$, and CO_2 calculation, $CO_{2Calculation}$, from TIC, pH, temperature, salinity and experimentally determined dissociation constants. *No measurements due to Easter.

Week	**Date**	**$CO_{2Franatech}$** [mg/L]	**$CO_{2Calculation}$** [mg/L]
9	26.02.2019	7.3	5.6
10	06.03.2019	6.5	5.6
11	14.03.2019	6.1	3.7
12	20.03.2019	6.4	3.5
13	28.03.2019	6.4	3.1
14	04.04.2019	7.0	3.6
15	09.04.2019	7.6	3.4
16*	-	-	-
17	26.04.2019	8.1	5.3
18	02.05.2019	8.0	3.2

TIC measurements were done only once a week. Hence, the concentration of CO_2 in the tank could only be calculated at this time. The reason for this was time-consuming analyzes, and that discrete TIC samples could not be collected and stored for later analysis. This was because TIC values in discrete water samples decreased with storing time which may originate from bacteria using CO_2 in their metabolism. Table 4.2 presents TIC values of 3 samples collected at 08:00, 10:00, and 12:00 the same day. The samples were analyzed right after collection (TIC_{0h}) and after 24 hours (TIC_{24h}). The concentration difference, Δ TIC, is also shown in the table.

Table 4.2: TIC concentration of samples collected at 08:00, 10:00, and 12:00 analyzed right after collection, TIC_{0h}, and after 24 hours after collection, TIC_{24h}. The concentration difference, Δ TIC, is also shown.

Sample	**Collection time**	**TIC_{0h}** [mg/L]	**TIC_{24h}** [mg/L]	**Δ TIC** [mg/L]
1	08:00	23.7	20.6	3.1
2	10:00	24.2	20.9	3.3
3	12:00	24.6	21.0	3.6

When calculating the CO_2 concentration, errors in TIC, pH, salinity and temperature measurements can result in inaccurate calculations. Erroneous measurements can be caused by sensor drift, change in solution from transit and storage, and inaccurate calibration. In Table 4.3, CO_2 calculation of a reference case of TIC = 20 mg/L, pH = 7, S = 13.0 ppt and T = 12 °C is shown in bold. Additionally, how changes of ± 1 mg/L TIC, ± 0.1 pH, ± 0.1 ppt S and ± 1 °C T affect the calculation are presented in the same table. Moreover, the experimentally determined dissociation constants were determined in seawater where the contribution from organic acids were neglected. This may also lead to uncertainties as various organic acids may be present in aquaculture. Example calculation for determining the CO_2 concentration are shown in Equation (B.1) to Equation (B.6) in Appendix.

Table 4.3: CO_2 calculations of a reference case of Total Inorganic Carbon (TIC) = 20 mg/L, pH = 7, salinity (S) = 13.0 ppt and temperature (T) = 12 °C, and how changes of ± 1 mg/L TIC, ± 0.1 pH, ± 0.1 ppt S and ± 1 °C T affects the calculation.

	TIC [mg/L]			**pH**			**S** [ppt]			**T** [°C]		
Value	19	**20**	21	6.9	**7.0**	7.1	12.9	**13.0**	13.1	11	**12**	13
CO_2	7.7	**8.3**	8.5	10.1	**8.3**	6.7	8.3	**8.3**	8.3	8.4	**8.3**	8.0

Reference measurements were also performed by classical titration with sodium hydroxide, and the results are presented in Table 4.4. Additional information for calculation the CO_2 concentration from the titration is given in Table B.2, Table B.3, Table B.4, Table B.5, Table B.6, Table B.7, Table B.8, Table B.9, Table B.10 and Table B.11 in Appendix. Example calculations to determine the concentration of the standard NaOH solution and CO_2 from the titration can be seen in Equation (B.7) and Equation (B.8) respectively in Appendix.

Table 4.4: Results from the classical titration with sodium hydroxide, $CO_{2Titration}$.

Week	**Date**	**$CO_{2Titration}$** [mg/L]
10	08.03.2019	8.8
12	22.03.2019	8.4
15	10.04.2019	8.1
17	25.04.2019	8.1
19	08.05.2019	9.1

Results from the classical titration can only be used as an approximation as there is are a lot of interference's with this method. In enclosed systems with significant biological activity, such as the RAS tank studied, various organic acid-base species are present which may result in errors in the standard titration. Concentrations determined by ICP-MS of filtrated water samples from the tank of phosporus, silicon and boron are shown in Table 4.5. If these elements were included in components with acid properties this may have resulted in a positive error in the classical titration. In addition, practical errors during the titration may also have affected the results. This include observation of the indicator endpoint and CO_2 loss of the CO_2 during transportation.

Table 4.5: Concentrations of some elements present in acid-base species in the water sample analyzed by ICP-MS.

Element	**Average concentration** [mg/L]
P	0.3
Si	1.7
B	1.4

Due to few reference measurements during the weeks of measurements with the SoluBlu sensor, visual evaluation of the data sets were mainly used for data analysis. Additionally, in two of the four parts of the experiment, water penetrated behind the sensor membrane which resulted in even less measurements for these two parts. It is important to remember that variability and uncertainty can occur from differences in the aquaculture system over the days.

4.2.2 Part 1: Teflon membrane

Measured concentration of carbon dioxide

In Part 1 of the experiment, the sensor was installed in the by-pass with the Teflon semipermeable membrane and open faced head. The measured variation of carbon dioxide concentration is shown in Figure 4.6 with error bars of $\pm$ 1 standard deviation of uncertainty showing every 7th hour (Enlarged: Figure B.1 in Appendix). The standard deviation was determined to be 1.10 mg/L. The red crosses are CO_2 concentrations calculated from TIC, salinity, temperature, pH and experimentally determined dissociation constants, the magenta circles are CO_2 measurements with the Franatech probe and the black diamond is the result from the classical titration with sodium hydroxide.

In this experiment, the measured CO_2 concentrations varied from 3.6 to 8.5 mg/L, while both CO_2 calculations were determined to be 5.6 mg/L. The two calculations of CO_2 lies within the error bars of the sensor measurements. One-Sample T-Tests showed that the sensor readings from the interval 30 minutes before and after the CO_2 calculation, on average, measured less than the determined value from CO_2 calculation; t(12)=-13, $p < 0.001$ and t(12)=-54, $p < 0.001$ (two-tailed) for the first and second CO_2 calculation respectively. The data set used to calculate test statistics for the second sampling significantly deviate from a normal distribution, and this may have affected the result. The two measurements from the Franatech probe and the result from the classical titration were above one standard deviation of the sensor measurement.

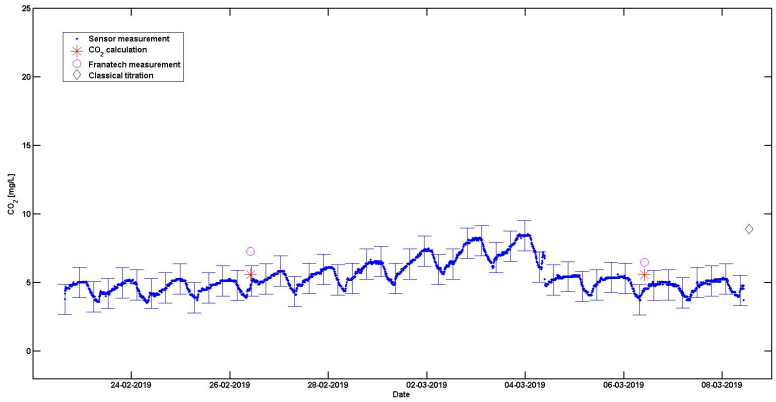

Figure 4.6: Variation of carbon dioxide concentration over a two week period measured with the open faced head with error bars of $\pm$ 1 standard deviation showing every 7th hour. The red crosses are CO_2 concentrations calculated from TIC, salinity, temperature and pH measurements, the magenta circles are CO_2 measurements with the Franatech probe and the black diamond is the result from the classical titration with sodium hydroxide.

In day 10 (04-03-2019) at around 09:00, the sedimentation in the bucket was removed by staff at Nofima. By looking at Figure 4.7, the sensor readings decrease from 7 mg/L at 09:25 to 4.9 mg/L at 09:35. This can be seen in the figure as a drop in CO_2 concentration (Enlarged: Figure B.2 in Appendix). As the sensor measure the concentration every fifth minute, the concentration change between two measurements are rarely above 0.1 mg/L. Thus, it is likely to believe that the drop in CO_2 concentration seen in the figure was a result of removing the sedimentation in the by-pass.

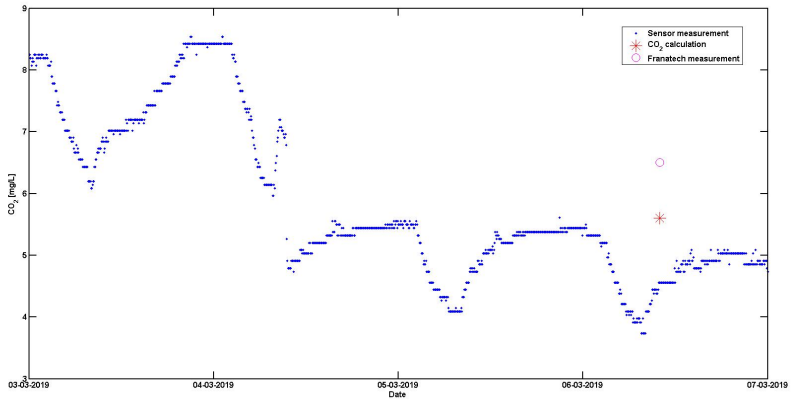

Figure 4.7: The event when sedimentation were removed from the bucked when measuring with the open faced head. The red cross is CO_2 concentration calculated from TIC, salinity, temperature and pH measurements and the magenta circle is CO_2 measurement with the Franatech probe.

After removing the sedimentation in the by-pass, it may look like the sensor readings went back to normal. A Friedman test showed that some of the measurement distributions from the first five days and after the by-pass was cleaned were the same with 0.05 significance level. The results of the test can be seen in Table B.13 in Appendix. This may be due to normal variations in the tank, but it can also strengthen the theory that the readings of the sensor went back to normal after the removing of sedimentation. Hence, removing the sedimentation in the bucked may work as a cleaning procedure to ensure reliable sensor output.

Qualitative estimate of biofouling

Due to the unexpected removal of sedimentation in day 10 of the experiment, photographs for a qualitative estimate of biofouling after two weeks could not be taken. However, photographs of the clean by-pass (a) and the by-pass after (b) four days are shown in Figure 4.8. Only after four days, sedimentation in the bucked and bioformation on the sensor housing and membrane could be observed. The fouling were easily removed from the sensor housing and membrane by a slow water circulation.

(a)

(b)

Figure 4.8: A clean by-pass (a) and the by-pass after four days (b) of the experiment using the Teflon membrane and open faced head.

Photographs of a clean Teflon membrane (a) and after four days in the by-pass (b) are shown in Figure 4.9.

(a) **(b)**

Figure 4.9: The clean Teflon membrane (a) and after four days (b) of part 1 of the experiment.

Photographs of the clean sensor housing (a) and after four days (b) of part 1 of the experiment are shown in Figure 4.10.

(a) **(b)**

Figure 4.10: The sensor housing before (a) and after (b) four days of part 1 of the experiment.

4.2.3 Part 2: Water-pumped flow-through head

Measured concentration of carbon dioxide

In Figure 4.11, the concentration of CO_2 is shown for the part of the experiment using the water-pumped flow-through head (Enlarged: Figure B.3 in Appendix). Error bars of $\pm$ 1 standard deviation were drawn every 7th hour from day 1 to day 11, and was determined to be 2.86 mg/L. The daily variation of CO_2 that was observed with the open faced head was not apparent when using this sensor head, and the reason why can only be discussed. The red crosses are CO_2 concentrations calculated from TIC, salinity, temperature, pH and experimentally determined dissociation constants, the red circles are measurements with the Franatech probe and the black diamonds are the result from the classical titration with sodium hydroxide.

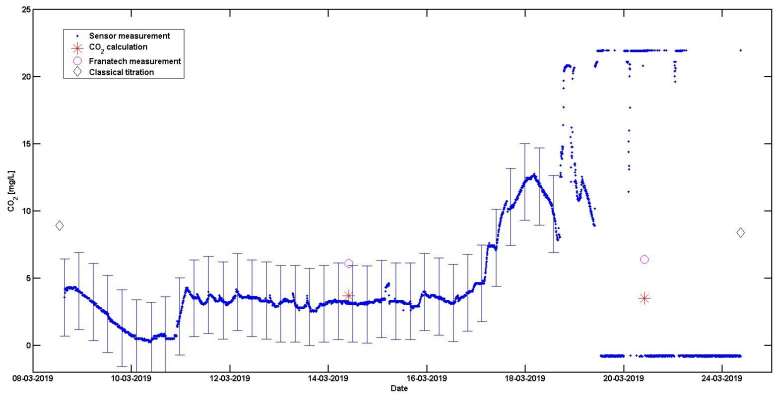

Figure 4.11: Variation of carbon dioxide concentration over a two week period with the water-pumped flow-through head. Error bars of $\pm$ 1 standard deviation are drawn every 7th hour. The red crosses are CO_2 concentrations calculated from TIC, salinity, temperature and pH measurements, the magenta circles are CO_2 measurements with the Franatech probe and the black diamonds are results from the classical titration with sodium hydroxide.

In this experiment, the measured CO_2 concentrations varied from 0 to 13 mg/L from day 1 to 11, while the first CO_2 calculation was determined to be 3.7 mg/L. The first calculation of CO_2 and Franatech measurement were within one standard deviation of the sensor measurement. One-Sample T-Test of sensors readings from the interval 30 minutes before and after the CO_2 calculation, on average, measured less than the determined value from CO_2 calculation; t(12)=-41, $p < 0.001$ (two-tailed). The data set used to calculate test statistics significantly deviate from a normal distribution, and this may have affected the result. The second reference measurement provided by these methods could not be compared to the sensor readings as the sensor was out of service.

The water flow in the hose transferring water to the pumped had was set to 1.5 L/min at Nofima instead of 0.3 L/min as the laboratory test were conducted with. This was due to that the probability of clogging the valve which controlled the water flow were high when

using 0.3 L/min. Additionally, it was recommended by Pro-Oceanus that a flow of 1-3 L/min should be used when attaching the pumped head. To prevent solid matter entering the hose transferring water to the pumped head, a filter could have been used in the inlet of the hose. This was not considered as an option because this filter would have required frequently cleaning to prevent clogging, and the amount of solid matter in the filter would have lead to a variable water flow entering the sensor head.

After two days (10-03-2019), the sensor measured the concentration of CO_2 to be 0 mg/L. This is an unlikely event in aquaculture, and may be a result of a temporary clogging of the water hose or a temporary biofilm formation on the membrane interface. Rapid changes in the environmental conditions of the water flowing towards the sensor may also result in sensor outputs at 0 mg/L as the sensor experience pressure waves due to turbulent waters. Another incident that may have resulted in the zero value is that the membrane was damaged and water has entered the infrared detector or electronics. As the readings increased back to normal values afterwards, it was assumed that no water had entered the infrared detector or electronics at this time.

After 10 days (19/03-19), the sludge collector in the tank was clogged. This resulted in a great amount of particular matter such as fish food, excrement and other particular matter flowed into the side wall drain of the fish tank which functioned as water supply for the sensor. This led to clogging of the water hose that transport water into the pumped head. This water hose was flushed by technicians at Nofima at 10:00 the same day to resolve the clogging. At the same time, the sensor readings increased from 10 mg/L to 20 mg/L in 5 minutes. It can be seen that the CO_2 measurements stabilized at 0 mg/L after this. Water was observed behind the membrane after removing the pumped head, and it is likely to believe that the high water pressure during the flushing resulted in movement in the membrane such that that water could penetrate behind the membrane. This indicate that the sensor was fragile towards pressure changes and particulate matter colliding with the membrane when using the pumped head.

The sensor showed increased values of CO_2 the day before the clogging, and this can be a result of particular matter colliding on the sensor membrane in the starting process of clogging in the sludge collector. This increase may also be due to other factors, such as natural variations in the water or a substantial layer of biofilm on the membrane interface.

Qualitative estimate of biofouling

Photographs of the pumped head (a) and sensor membrane (b) are shown in Figure 4.12 after 30 minutes washing with fresh water. It can be seen that even after washing with tap water, particular matter was still retained in the sensor head. Additionally, a pellet was stuck in one of the pipes carrying water into or out of the sensor head. Pellets stuck in the hose may have contributed to creating an uneven water flow. The housing of the sensor was not affected by fouling as it was not immersed into water.

(a) **(b)**

Figure 4.12: The Water-pumped flow-through head (a) and Teflon membrane (b) after part 2 of the experiment. The head was washed with tap water for 30 minutes before detaching the pumped head.

4.2.4 Part 3: Copper grid

Measured concentration of carbon dioxide

For part 3 of the experiment, a copper grid was placed between the Teflon membrane and the open faced head. The grid size was designed to be small enough to have an optimal biocidal effect while big enough for biomass not to get stuck in the grid. Especially, if the pump head was to be used together with the copper grid, it would be important that the copper grid should not work as a filter to collect particular matter. The results from this part of the experiment are shown in Figure 4.13 (Enlarged: Figure B.4 in Appendix). Error bars of $\pm$ 1 standard deviation are showing every 7th hour. The standard deviation was determined to be 1.45 mg/L. The red crosses are CO_2 concentrations calculated from TIC, salinity, temperature, pH and experimentally determined dissociation constants, the magenta circles are measurements with the Franatech probe and the black diamonds are the result from the classical titration with sodium hydroxide.

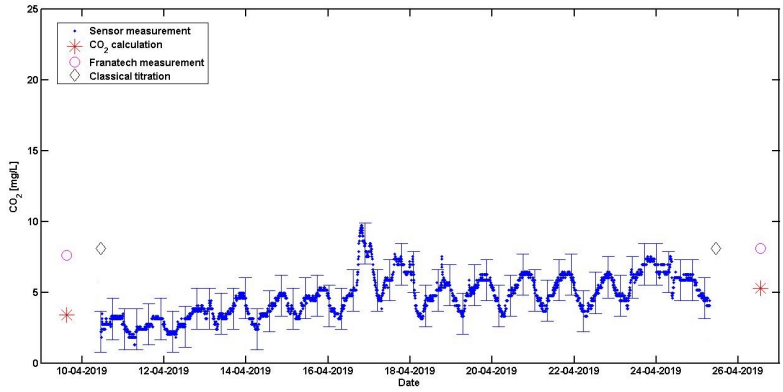

Figure 4.13: Variation of carbon dioxide concentration over a two week period measured with the copper grid. Error bars of $\pm$ 1 standard deviation are showing every 7th hour. The red crosses are CO_2 concentrations calculated from TIC, salinity, temperature and pH measurements, the magenta circles are CO_2 measurements with the Franatech probe and the black diamond is the result from the classical titration with sodium hydroxide.

In this experiment, the measured CO_2 concentrations varied from 1.3 to 9.7 mg/L. Unfortunately, no CO_2 calculations or Franatech measurements were done during the experiment with the copper grid due to Easter holiday. However, both CO_2 calculations and Franatech measurements were done the day before and the day after sensor measurements. It can be seen that the output values of the sensor increases with time, and this can be due to an increase in the water from the tank as both the CO_2 calculation and Franatech measurement shows higher values in the end of the measuring period than in the beginning of the measuring period.

After 6 days (16-04-2019) the CO_2 measurements suddenly increase in a two day period. It was not reported any incidents which may explain this increase in the fish tank.

Qualitative estimate of biofouling

Pictures of the by-pass with the sensor after (a) 1 and (b) 2 weeks can be seen in Figure 4.14. The pictures were taken with different cameras, hence the change in color in the pictures. The amount of biofouling on the sensor and the plastic object looked to be of same character.

(a)

(b)

Figure 4.14: Photographs of the by-pass with the sensor after (a) 1 week and (b) 2 weeks. The photographs were taken with different cameras, thus the quality and color were different.

Figure 4.15 shows the fouling on the membrane behind the copper grid after two weeks.

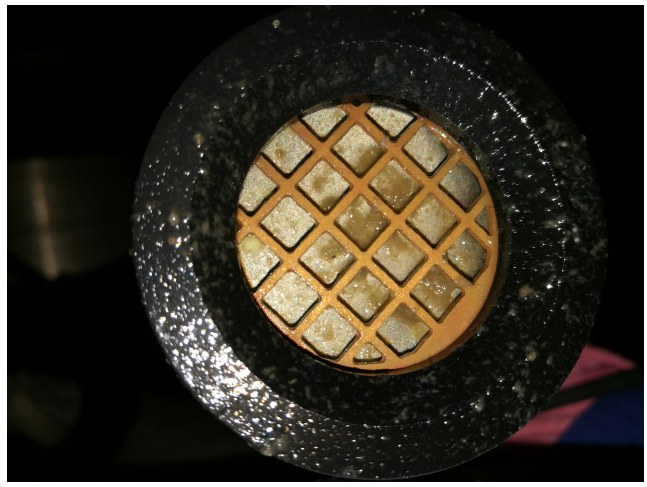

Figure 4.15: Fouling on the membrane behind the copper grid after two weeks.

4.2.5 Part 4: Polydimethylsiloxane (PDMS) membrane

Measured concentration of carbon dioxide

In Part 4 of the experiment, the sensor was installed in a by-pass using both the PDMS membrane and the Teflon membrane. The measured variation of carbon dioxide concentration for this part of the experiment is shown in Figure 4.16 with error bars of $\pm$ 1 standard deviation calculated from day 1 to 7 showing every 7th hour (Enlarged: Figure B.5 in Appendix). The standard deviation was determined to be 0.87 mg/L for this period. The red crosses are CO_2 concentrations calculated from TIC, salinity, temperature, pH and experimentally determined dissociation constants, the magenta circles are measurements with the Franatech probe and the black diamonds are the result from the classical titration with sodium hydroxide.

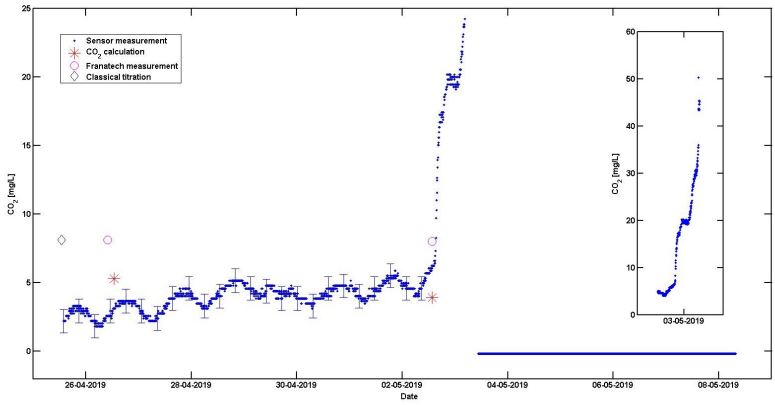

Figure 4.16: Variation of carbon dioxide concentration over a two week period measured with the PDMS membrane together with the Teflon membrane. Error bars of $\pm$ 1 standard deviation are drawn every 7th hour. The red crosses are CO_2 concentrations calculated from TIC, salinity, temperature and pH measurements, the magenta circles are CO_2 measurements with the Franatech probe and the black diamonds are the result from the classical titration with sodium hydroxide.

In this experiment, the measured CO_2 concentrations varied from 1.8 to 5.9 mg/L from day 1 to 7, while the two CO_2 calculations were determined to be 5.3 and 3.2 mg/L. All of the reference measurements were not within within the error bars of $\pm$ 1 standard deviation. This may be due to the long response time when using the two membranes which result in less oscillation in the concentration range. One-Sample T-Tests shows that the sensor readings from the interval 30 minutes before and after the CO_2 calculation, on average, measured less or more than the determined value from CO_2 calculation; t(12)=-154 and t(12)=66 for p = 0.05 (two-tailed) for the first and second CO_2 calculation respectively. The data set used to calculate both test statistics significantly deviated from a normal distribution, and this may have affected the result.

Friday 03-04-2019 at 15.30, the measurements increased rapidly before they stabilized at 0 mg/L CO_2. The full increase is shown in the addition graph in Figure 4.16. When removing the membranes, water was observed behind the Teflon membrane. It was also observed that the PDMS membrane had sticked to the underlying Teflon membrane, resulting in no air between the membranes. It is likely to believe that water infiltrated the sensor when the measurements started to increase because same chain of events could be seen with the pumped head when water infiltrated behind the membrane. The reason why the PDMS membrane was sticked to the Teflon membrane after two weeks might be due to differences in the permeability and thickness of the membranes. Whether this had a role in the event of water entering the sensor can only be discussed.

Qualitative estimate of biofouling

Figure 4.17 shows fouling on the sensor membrane (a) and housing (b) after two weeks of part 4 of the experiment.

(a) **(b)**

Figure 4.17: Fouling on the sensor membrane (a) and housing (b) after two weeks measuring at Nofima.

Figure 4.18 shows sedimentation in the by-pass after two weeks of the experiment. The fouling was easily removable.

Figure 4.18: Sedimentation in the by-pass after two weeks of the experiment.

4.2.6 Daily variation of carbon dioxide concentration

In aquaculture, carbon dioxide cycle daily mainly due to respiration. In some cases, it is interesting to monitor the fluctuation of CO_2 during one daily cycle. By using Equation (2.31) the daily CO_2 increase in the studied tank was estimated to be 2.4 mg/L. Calculation can be seen in Equation (B.9) in Appendix. There are several factors that may result in a larger or smaller daily increase, such as heterotrophic and autotrophic bacteria. If heterotrophs were present in the by-pass they may increase the concentration of CO_2, while autotrophs may decrease the concentration of CO_2 during the period of light and affect the measurements. The by-pass was placed underneath the side-wall drain, hence it is expected that a minimum of light reached the by-pass. Further, some of the feed may end up in the sludge collector and not consumed by the fish resulting in less CO_2 produced.

Figure 4.19 shows the daily variation of the carbon dioxide concentration from 16:00 in the first day, to 16:00 in the second day for all four parts of the experiment (Enlarged: Figure B.6 in Appendix). The first measurement in all cases were shifted to a starting value at 4.5 mg/L to make it easier to compare. The Matlab script for creating the plot can

be seen in Listing C.3 in Appendix.

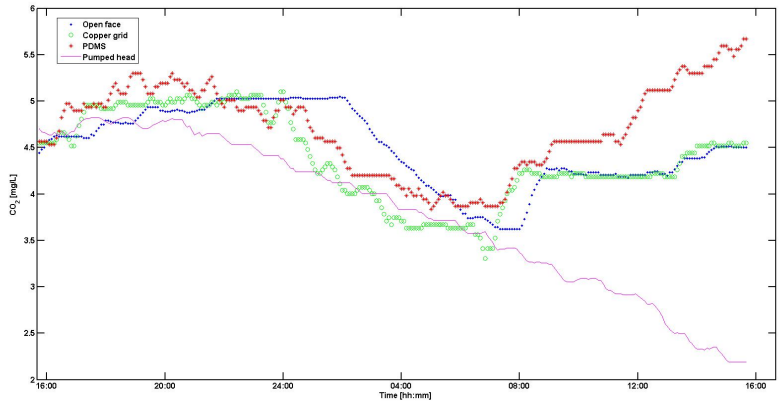

Figure 4.19: The carbon dioxide concentration variation through 24 hours for all of the four different antifouling mechanisms.

As found by Hoar, and presented in the theory, the fish start their feeding activity after the light is turned on at 08:00. This is also the time when the fish are starting to receive food. The feeding activity is more intensive in the morning hours than in the evening, and there is a mid-day depression from 10:00. Further, the fish shows a nocturnal depression. This pattern were observed for all the measurements with a variable degree, except when using the water-pumped flow-through head. CO_2 calculations presented in Table 4.6 also shows an increase in CO_2 concentration from 08:00, 10:00 and 12:00 during one day. Samples from 14:00 and 16:00 were also collected, but not analyzed before the next day due to working hours at the Nofima laboratory. This resulted in a change in CO_2 concentration due to storing. Measurements used to calculate the CO_2 concentrations can be seen in Table B.14 in Appendix in addition to the samples analyzed after 24 hours.

Table 4.6: Calculated CO_2 concentration of samples collected at 08:00, 10:00, and 12:00 the same day.

Sample	**Collection time**	**CO_2** [mg/L]
1	08:00	5.3
2	10:00	5.8
3	12:00	6.1

The reason why the sensor captured a great dynamic range during a daily cycle for all parts of the experiment except for when using the water-pumped flow-through head may be due to various reasons. Sensitivity towards pressure changes and particles colliding with the sensor membrane when using the pumped head can be a reason for this. For analyzes of discrete water samples, the daily cycle shows that it is important to collect samples from the same time of day to ensure comparable results.

4.2.7 Polynomial curve fitting

Polynomial curves were created from sensor measurements from day 3 to 6 for all four parts of the experiment. This was the only time when the sensor gave reasonable output for all four parts of the experiment. Further, biofouling growth on equipment in aquaculture are often observed after approximately three days. The polynomials and maximum of the absolute value of the deviation of the data are presented in Table 4.7. The max error was smaller than any of the data values for all polynomials which indicate good models.

For validating the models, the models were plotted together with the original data. This can be seen in Figure 4.20 for the (a) open face, (b) pumped head, (c) copper grid and (d) pumped head. (Enlarged versions for the open faced head, copper grid, pumped head and PDMS membrane can be seen in Figure B.7, Figure B.8, Figure B.9 and Figure B.10 respectively in Appendix.)

Table 4.7: The polynomials created from day 3 to 6 for the four parts of the experiment together with the maximum of the absolute value of the deviation of the data.

Antifouling mechanism	**Polynomial**	**Max Error**
Open face	$9.2 \cdot 10^{-7}x^2$ - $1.4 \cdot 10^{-3}x + 5.4$	1.2
Pumped head	$1.1 \cdot 10^{-6}x^2$ - $3.4 \cdot 10^{-3}x + 5.8$	0.73
Copper grid	$1.0 \cdot 10^{-6}x^2$ - $1.8 \cdot 10^{-3}x + 4.6$	1.5
PDMS	$2.8 \cdot 10^{-6}x^2$ - $7.8 \cdot 10^{-3}x + 9.7$	1.0

A Kruskal-Wallis H test showed that there was a statistically significant difference in CO_2 concentration between measurements with the different antifouling mechanisms during day 3 to 6, $\chi^2(3) = 2325$, $p < 0.05$, with a mean rank CO_2 concentration of 2897, 1918, 1648 and 579 for the open faced head, PDMS membrane, copper grid and pumped head respectively. The total ranks were 3520.

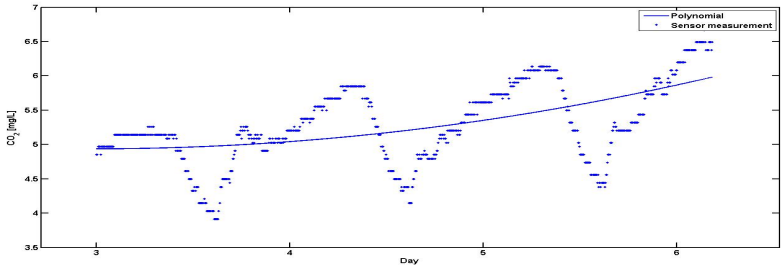

(a)

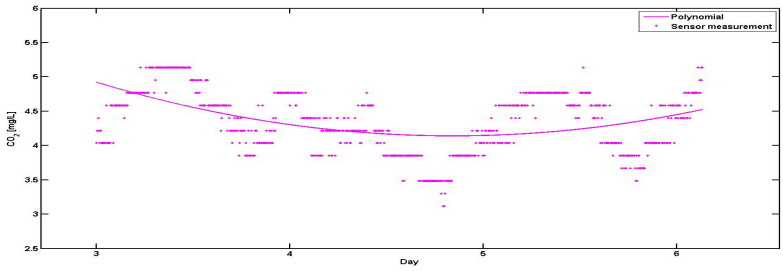

(b)

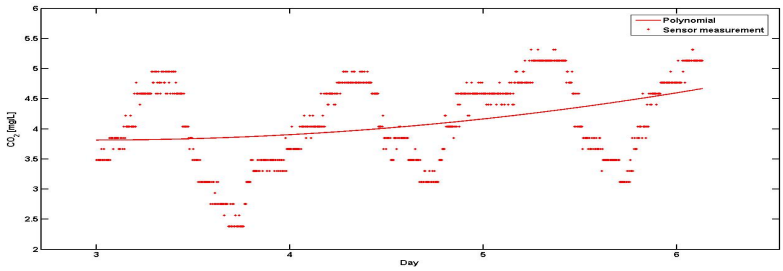

(c)

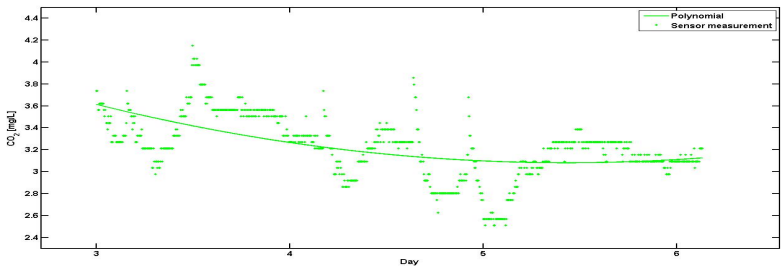

(d)

Figure 4.20: Original data and model were plotted together for (a) open faced head, (b) pumped head, (c) copper grid, and (d) PDMS membrane.

All of the polynomials are plotted together in Figure 4.21 (Enlarged: Figure B.11 in Appendix). The concentration of CO_2 increase with successive days when using the open faced head and copper grid. The Matlab script for creating the plot can be seen in Listing C.2 in Appendix. The reference calculation of CO_2 when using the open faced head showed no increase from day 5 to day 13 which may indicate that the increase of CO_2 is due to biofouling. On the other hand, the reference calculation of CO_2 showed an increase in CO_2 concentration from 3.4 mg/L the day before measurements to 5.3 mg/L the day after measurements when using the copper grid. This may mean that the measured increase wasn't necessarily due to biofouling but may been due to an increase in the tank during these days.

The reference calculation of CO_2 showed a decrease in CO_2 concentration from 5.3 mg/L in day 2 to 3.9 mg/L in day 8 when using the PDMS membrane. The decrease in sensor readings may mean that the flattening of the curve may be due to a decrease of CO_2 in the tank.

The shape of the curve for the pumped head is decreasing, and it is hard to interpret the measurements from this experiment. The reference calculation of CO_2 showed a decrease in CO_2 concentration from 5.6 mg/L two days before measurement to 3.7 in day 7.

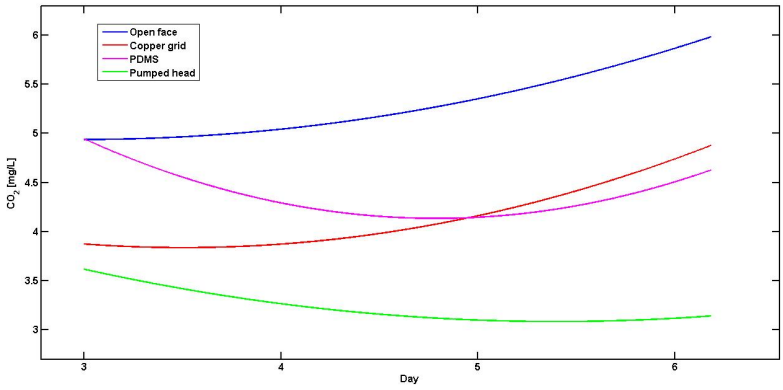

Figure 4.21: Polynomial curve fitting of second degree for the four data sets. The blue, red, magenta and green line correspond to the curve of open face, copper grid, PDMS membrane and pumped head respectively.

4.2.8 Water penetrating behind the sensor membrane

After using the pumped head and the PDMS membrane, water were observed behind the sensor membrane. Figure 4.22 show the sensor readings when this event probably happened for these two cases (Enlarged: Figure B.12 in Appendix). During the incident, the maximum sensor reading was approximately 22 and 50 mg/L using the pumped head and PDMS membrane respectively. The reason why water penetrated behind the sensor membrane when using the pumped head was unclogging of the water hose transferring water to the head. This created a relatively great pressure resulting in water accessing behind the sensor membrane. On the other hand, it it uncertain how water penetrated behind the sensor membran when using the PDMS membrane. However, the PDMS membrane was sticked to the underlying Teflon membrane after the experiment. This may be a result of different permeability and thickness of the two membranes. Whether this was a factor for how water accessed inside of the sensor can only be discussed.

After several days of drying and testing, the sensor started working again after the pumped head was used. On the other hand, the sensor did not respond to differences in CO_2 concentration after the experiment with the PDMS membrane. The different sensor measurements indicate that the water infiltrated the sensor in different ways in the two experiments which may resulted in the different outcomes. The sensor was opened in both cases, and the electronics looked unharmed by both incidents.

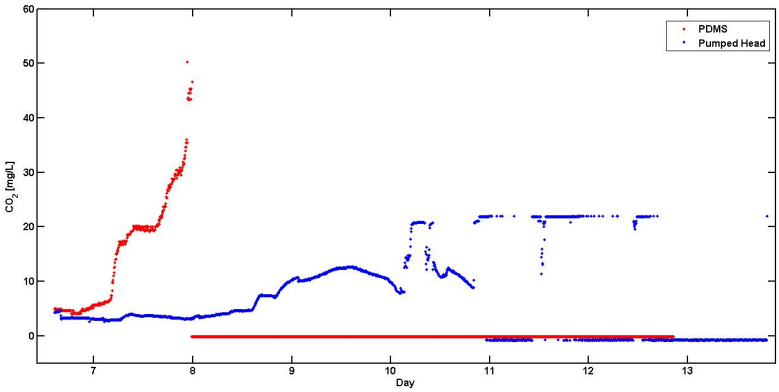

Figure 4.22: Measured concentration of CO_2 during the incident when water penetrated behind the sensor membrane when using the pumped head and PDMS membrane.

Chapter 5

Conclusion

The Pro-Oceanus Solu-Blu sensor proved to be suitable for in situ measurements in aquaculture with continuously monitoring and logging. However, when the sensor was used in Recirculating Aquaculture Systems (RAS) at Nofima, the readings were significantly different from the calculated CO_2 concentrations evaluated by One-Sample T-Tests. Differences may origin from a number of factors including uncertainties in the reference and comparison process, how well the sensor was set up, errors in the reference measurement, and the sensor error among others. The data sets used in the One-Sample T-Tests were not completely in agreement with the assumptions of the test such as approximately normal distributed data and independent samples which may have resulted in errors.

A limitation of this study was few reference measurements. More reference measurements have to be conducted to conclude if the Solu-Blu CO_2 sensor measured the real concentration in the water, or if the sensor readings were affected by bifouling. A possible further study is to analyze simultaneously with several of the same sensors using different antifouling mechanisms to avoid the variability and uncertainty of CO_2 changes in the water over time.

Biofilms were formed rapidly on the surface of the sensor housing and membrane in all cases. In addition, a layer of sedimentation quickly settled in the by-pass. The biofilms formed on the sensor housing and membrane were easily removed. Just a swirl in the water removed most of the fouling, and thus the washing procedure involving a small water circulation was sufficient in this experiment.

Removing of the sedimentation in the by-pass after 10 days resulted in a drop in CO_2 concentration when using the Teflon membrane and open faced head. This indicated that the measurements were affected by biofouling.

During day 3 to 6, measurements with the copper grid and the Teflon membrane increased with successive days. This could be a result of biofouling or CO_2 increase in the tank. Further studies may involve Scanning Electron Microscope (SEM) analysis to evaluate the biofouled membranes. In addition, different design of the copper grid such as grid size and thickness of the grid can be tested. The measurements with the PDMS membrane and pumped head did not show the same increase during day 3 to 6, and it is less likely

that these measurements were affected by biofouling.

A dynamic range was captured during a daily cycle when using all antifouling mechanisms except for the pumped head. The reason for this may be that the membrane is sensitive towards particles such as pellets colliding with the membrane when using the pumped head. Water pressure created by flushing the hose transferring water to the pumped head resulted in water penetrating under the sensor membrane. If the liquid to be analyzed in do not contain large dissolved or solid particles, more experiments can be conducted with the pumped head. Further, different water flows can be tested to find the optimal flow rate into the head.

The reason why water penetrated behind the sensor membrane when testing the PDMS membrane is uncertain. The PDMS membrane used in this study had a variable thickness, variating from 1 to 2 mm. Further work can be done to see if a thinner and more uniform PDMS membrane can be completely exchanged with the Teflon membrane. Additionally, as membrane technology is promising, other membranes can be tested to assess antifouling efficiency.

The Pro-Oceanus Solu-Blu sensor measured the dissolved CO_2 in the water directly, and did not require additional calculations such as the CO_2 calculation from TIC, salinity, temperature, pH and experimentally determined dissociation constants. The method of CO_2 calculation may also suffer from loss of CO_2 during sample collection, transit, and analysis whereas NDIR detectors do not. In addition, the CO_2 calculation include uncertainties in measurement of Total Inorganic Carbon (TIC), salinity and pH which can affect the accuracy of the calculation. A slight change in pH due to drifting of the pH meter can have a substantial effect on the CO_2 calculation. However, sensors measuring pCO_2 are typically quite expensive.

The classical titration method has several sources of error and could only be used for estimation, and showed higher levels of CO_2 than measurements with the three other methods. In the laboratory, classical titrations of CO_2 spiked water can be compared with sensor readings. This is a more reliable comparison as aquacultural water contain various organic acid-base species which may result in errors in the titration. The Franatech solid state detector showed higher CO_2 values than both CO_2 caluclation and the Solu-Blu sensor.

Both the logging cabinet and the deck box were tested for measurements with the sensor. The deck box only needed salinity input, while the logging cabinet needed inputs for temperature, total gas pressure, and salinity. Average values for these parameters were inserted, and this may have been a source of error when the real value differed from the average value. In addition, the logging cabinet saved the measurements on a memory stick, which was a bit more cumbersome then transferring the output directly to a computer which was done by the deck box.

Bibliography

Atamanchuk, D., Tengberg, A., Thomas, P. J., Hovdenes, J., Apostolidis, A., Huber, C., and Hall, P. O. (2014). Performance of a lifetime-based optode for measuring partial pressure of carbon dioxide in natural waters. *Limnology and Oceanography: Methods*, 12(2):63–73.

Banica, F.-G. (2015). *KJ 2050: Laboratory course - Excercise No. 1*. Norwegian University of Science and Technology (NTNU), Høgskoleringen 5, Trondheim, Norway, 1 edition.

Blackman, A. (2014). *Aylward and Findlay's SI Chemical Data*. John Wiley and Sons, Milton, Queensland, 7 edition.

Chadwick, M. P., Parsons, G. J., and Sayavong, B. (2010). *Evaluation of closed-containment technologies for saltwater salmon aquaculture*. NRC Research Press, Ottawa.

CHEMetrics (2012). *Technical Data Sheet - Carbon dioxide (dissolved)*. CHEMetrics Inc., 4295 Catlett Road, Midland, VA.

Cronin, E. R., Cheshire, A. C., Clarke, S. M., and Melville, A. J. (1999). An investigation into the composition, biomass and oxygen budget of the fouling community on a tuna aquaculture farm. *Biofouling*, 13(4):279–299.

Delauney, L., Compere, C., and Lehaitre, M. (2010). Biofouling protection for marine environmental sensors. *Ocean Science*, 6(2):503–511.

Dickson, A. (2010). The carbon dioxide system in seawater: Equilibrium chemistry and measurements. *Guide to Best Practices for Ocean Acidification Research and Data Reporting*, pages 17–40.

Dickson, A. G., Sabine, C. L., and Christian, J. R. (2007). Guide to best practices for ocean carbon dioxide measurement. ICES Special Publication 3, 191 pp.

Dürr, S. and Thomason, J. C. (2009). *Biofouling*. Blackwell, Ames, Iowa, 1 edition.

Fietzek, P., Fiedler, B., Steinhoff, T., and Körtzinger, A. (2014). In situ quality assessment of a novel underwater pCO_2 sensor based on membrane equilibration and ndir spectrometry. *Journal of Atmospheric and Oceanic Technology*, 31(1):181–196.

Fietzek, P. and Körtzinger, A. (2010). Optimization of a membrane-based ndir sensor for dissolved carbon dioxide. In Hall, J., Harrison, D. E., and Stammer, D., editors, *Sustained Ocean Observations and Information for Society Conference*, ESA Publication, pages 1–4. OceanObs'09, Venice, Italy. Annex.

Good, C., Davidson, J., Terjesen, B., Takle, H., Kolarevic, J., Bæverfjord, G., and Summerfelt, S. (2018). The effects of long-term 20 mg/l carbon dioxide exposure on the health and performance of atlantic salmon salmo salar post-smolts in water recirculation aquaculture systems. *Aquacultural Engineering*, 81:1–9.

Gouveia, C., Markovics, A., Baptista, J., Kovacs, B., and Jorge, P. (2010). Measurement of CO_2 using refractometric fiber optic sensors. pages 169–173. Proceedings of the 3rd WSEAS international conference on Advances in sensors, signals and materials.

Hach (2015). *Carbon Dioxide - Sodium Hydroxide Method*. Hach Company/Hach Lange GmbH, Loveland, Colorado, 80539-0389, 8 edition.

Herrón, J., Mandayo, G. G., and o, E. C. (2009). Semiconducting $BaTiO_3$-CuO mixed oxide thin films for CO_2 detection. volume 517, pages 6192 – 6197. Proceedings of VI International Workshop on Semiconductor Gas Sensors - SGS 2008.

Hoar, W. S. (1942). Diurnal variations in feeding activity of young salmon and trout. *Journal of the Fisheries Research Board of Canada*, 6a(1):90–101.

Jiang, Z.-P., J. Hydes, D., Hartman, S., Hartman, M., Campbell, J., D. Johnson, B., Schofield, B., Turk, D., Wallace, D., Burt, W., Thomas, H., Cosca, C., and Feely, R. (2014). Application and assessment of a membrane-based pCO_2 sensor under field and laboratory conditions. *Limnology and oceanography, methods*, 12:264–280.

Metcalfe, N. B., Fraser, N. H. C., and Burns, M. D. (1998). State-dependent shifts between nocturnal and diurnal activity in salmon. volume 265, pages 1503–1507.

Millero, F. J., Pierrot, D., Lee, K., Wanninkhof, R., Feely, R., Sabine, C. L., Key, R. M., and Takahashi, T. (2002). Dissociation constants for carbonic acid determined from field measurements. *Deep Sea Research Part I: Oceanographic Research Papers*, 49(10):1705 – 1723.

Moran, D., Tirsgård, B., and Steffensen, J. F. (2010). The accuracy and limitations of a new meter used to measure aqueous carbon dioxide. *Aquacultural Engineering*, 43(3):101–107.

Morrissey, J., Sumich, J., and Pinkard-Meier, D. (2016). *Introduction to the Biology of Marine Life*. Jones & Bartlett Learning, Burlington.

Mota, V. C., Nilsen, T. O., Gerwins, J., Gallo, M., Ytteborg, E., Baeverfjord, G., Kolarevic, J., Summerfelt, S. T., and Terjesen, B. F. (2019). The effects of carbon dioxide on growth performance, welfare, and health of atlantic salmon post-smolt (salmo salar) in recirculating aquaculture systems. *Aquaculture*, 498:578 – 586.

Nofima (2019). Nofima centre for recirculation in aquaculture. [Online] Available at: https://nofima.no/en/research-facilities/nofima-centre-for-recirculation-in-aquaculture/, (Accessed: 12. april 2019).

Pedersen, B. (2018). Henryloven. [Online]. Available at : https://snl.no/Henryloven, (Accessed 31. may 2019).

Pro-Oceanus (2016). *Pro-Oceanus CO2-Pro CV User's Manual*. Pro-Oceanus Systems Inc., 80 Pleasant Street, Bridgewater, Nova Scoatia, Canada, B4V 1N1. Revision 3.0.3.

Pro-Oceanus (2018). *Pro-Oceanus Solu-Blu CO2 User's Manual*. Pro-Oceanus Systems Inc., 80 Pleasant Street, Bridgewater, Nova Scoatia, Canada, B4V 1N1. Revision 1.0.0.

Randall, D. J. and Wright, P. A. (1987). Ammonia distribution and excretion in fish. *Fish Physiology and Biochemistry*, 3(3):107–120.

Reggiani, E. R., Bellerby, R. G. J., and Sørensen, K. (2014). Underwater spectrophotometric detection: Scaling down ocean acidification monitoring. In *2014 IEEE Sensor Systems for a Changing Ocean (SSCO).*, pages 1–5.

Sankar, G. G., Sathya, S., Murthy, P. S., Das, A., Pandiyan, R., Venugopalan, V., and Doble, M. (2015). Polydimethyl siloxane nanocomposites: Their antifouling efficacy in vitro and in marine conditions. *International Biodeterioration and Biodegradation*, 104:307 – 314.

Shukla, A. K., Alam, J., Alhoshan, M., Arockiasamy, L., and R. Muthumareeswaran, M. (2017). Development of a nanocomposite ultrafiltration membrane based on polyphenylsulfone blended with graphene oxide. *Scientific Reports*, 7:41976.

Skoog, D. A. (2007). *Principles of instrumental analysis*. Thomson Higher Education, Belmont, Calif, 6th ed., international student ed. edition.

SPSS (2018a). Friedman test in spss statistics. [Online]. Available at: https://statistics.laerd.com/spss-tutorials/friedman-test-using-spss-statistics.php, (Accessed 09. June 2019).

SPSS (2018b). Kruskal-wallis h test using spss statistics. [Online]. Available at: https://statistics.laerd.com/spss-tutorials/kruskal-wallis-test-using-spss-statistics.php, (Accessed 09. June 2019).

SPSS (2018c). One-sample t-test using spss statistics. [Online]. Available at: https://statistics.laerd.com/spss-tutorials/one-sample-t-test-using-spss-statistics.php, (Accessed 13. June 2019).

SPSS (2018d). Testing for normality using spss statistics. [Online]. Available at: https://statistics.laerd.com/spss-tutorials/testing-for-normality-using-spss-statistics.php, (Accessed 13. June 2019).

Stiller, K., Vanselow, K., Moran, D., and Schulz, C. (2014). Available technologies for CO_2 measurements in ras. 3rd conference in recirculation of water in aquaculture: Future smolt production, Sunndalsøra, Norway, 22.-23.10.2014.

TheMathWorks (2014a). Filtering and smoothing data. Matlab documentation center.

TheMathWorks (2014b). Polyfit - polynomial curve fitting. Matlab documentation center.

ThermoFisherScientific (2008). *Users Guide: Carbon Dioxide Ion Selective Electrode*. Thermo Fisher Scientific Inc., 166 Cummings Center, Beverly, MA 01915 USA.

Thomas, R. (2004). *Practical guide to ICP-MS*, volume 33 of *Practical spectroscopy*. Marcel Dekker, New York.

Timmons, M. B. and Ebeling, J. (2007). *Recirculating aquaculture*. Cayuga Aqua Ventures, Ithaca, N.Y. xviii, 975 p.

Turley, C., Nightingale, P., Riley, N., Widdicombe, S., Joint, I., Gallienne, C., Lowe, D., Goldson, L., and Beaumont, N. (2004). Literature review: environmental impacts of a gradual or catastrophic release of CO_2 into the marine environment following carbon dioxide capture. *Report to the UK Department for Environment*.

Voulvoulis, N., Scrimshaw, M. D., and Lester, J. N. (1999). Alternative antifouling biocides. *Applied Organometallic Chemistry*, 13(3):135–143.

Walpole, R. R., Myers, R. H., Myers, S. L., and Ye, K. (2012). *Probability & Statistics for Engineers & Scientists*. Pearson Education, 9. edition.

Wolf-Gladrow, D. A., Zeebe, R. E., Klaas, C., Körtzinger, A., and Dickson, A. G. (2007). Total alkalinity: The explicit conservative expression and its application to biogeochemical processes. *Marine Chemistry*, 106(1):287 – 300.

Wu, X., Zheng, L., and Wu, D. (2005). Fabrication of superhydrophobic surfaces from microstructured zno-based surfaces via a wet-chemical route. *Langmuir*, 21(7):2665–2667. PMID: 15779932.

Yoon, T. K., Jin, H., Oh, N. H., and Park, J. H. (2016). Technical note: Assessing gas equilibration systems for continuous pCO_2 measurements in inland waters. *Biogeosciences*, 13(13):3915–3930.

Zeebe, R. and Wolf-Gladrow, D. (2001). *CO_2 in Seawater: Equilibrium, Kinetics, Isotopes*, volume 65 of *Elsevier Oceanography Series*. Elsevier Science, Amsterdam.

Zosel, J., Oelßner, W., Decker, M., Gerlach, G., and Guth, U. (2011). The measurement of dissolved and gaseous carbon dioxide concentration. *Measurement Science and Technology*, 22(7):072001.

Appendix

A Laboratory testing

i) Measurements with the Solu-Blu sensor

Following are enlarged versions of the graphs presented in section 4.1. The laboratory test comparing sensor readings when using the pumped head and the open face head, and with and without the copper grid can be seen in Figure A.1 and Figure A.2 respectively. Further, the concentration change of a spiked CO_2 solution over time can be seen in Figure A.3. The laboratory test comparing sensor readings with the Teflon and polydimethylsiloxane (PDMS) membrane is presented in Figure A.4. How an air bubble accumulated on the membrane interface affect sensor readings is presented in Figure A.5.

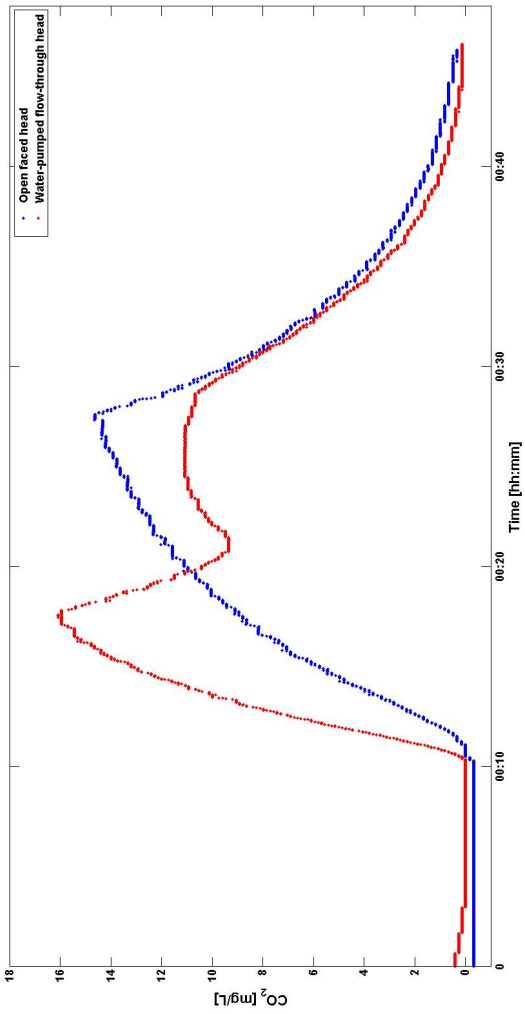

Figure A.1: Sensor readings when testing the pumped head and open faced head. The experiments were performed 10 minutes in tap water, 20 minutes in CO2 spiked water, and 20 minutes in tap water.

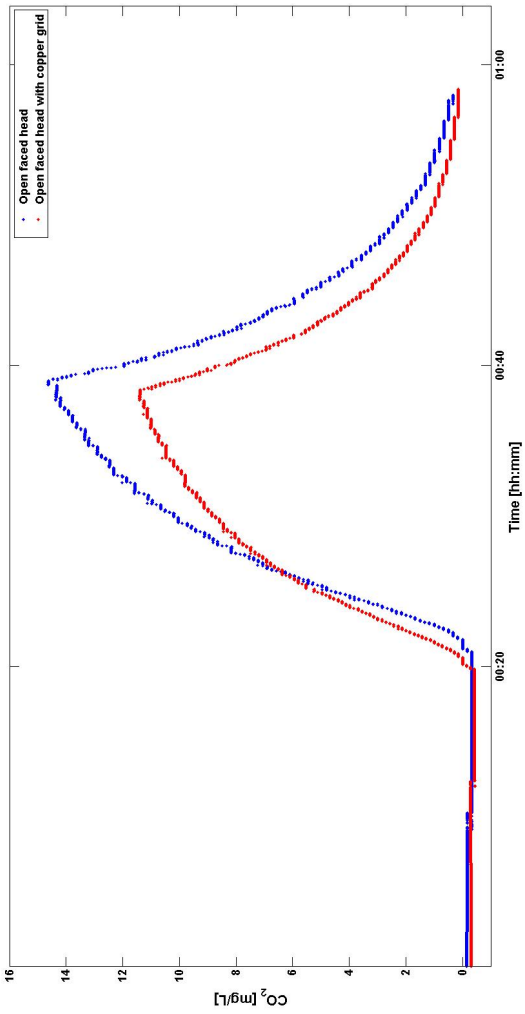

Figure A.2: Sensor readings when testing the sensor with and without the copper grid in the laboratory. The tests were performed 10 minutes in tap water, 20 minutes in CO_2 spiked water, and then 20 minutes in tap water.

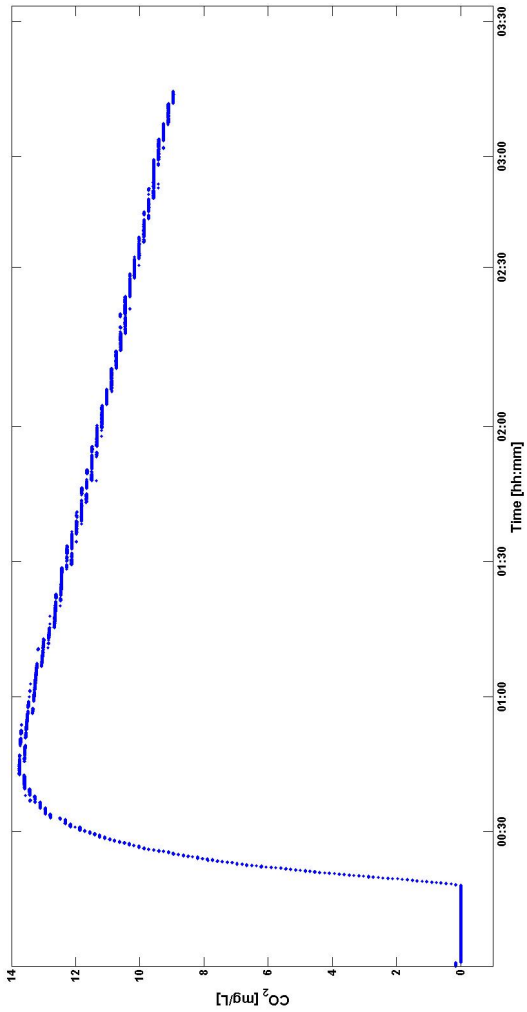

Figure A.3: The concentration change of a spiked CO_2 solution over time. The experiment was performed 20 minutes in tap water and then over 3 hours in CO_2 spiked water.

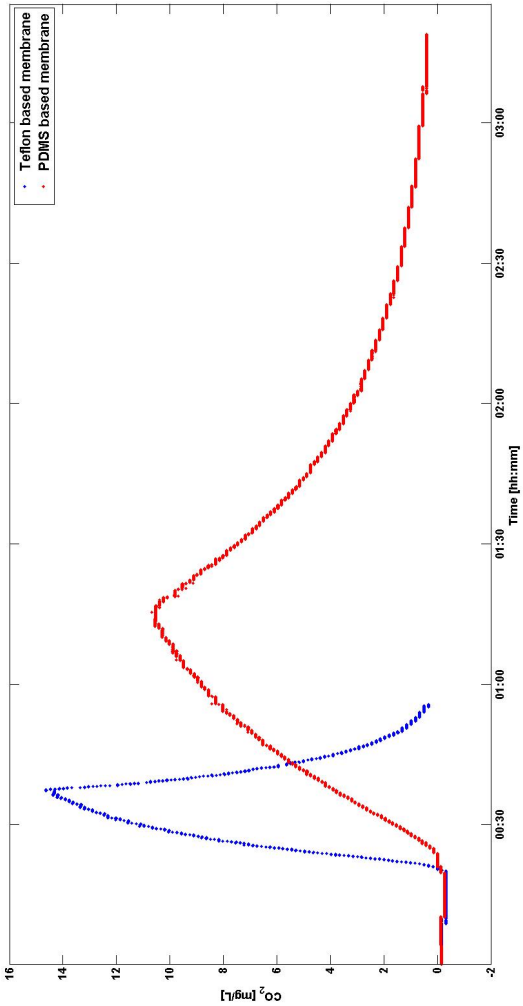

Figure A.4: Response times for the Teflon membrane and the polydimethylsiloxane (PDMS) membrane together with the Teflon membrane in laboratory conditions. After 20 minutes in tap water, the sensor was moved to a CO_2 spiked solution in both experiments. For the Teflon membrane, the experiment was performed 20 minutes in the CO_2 spiked solution before it was moved back to tap water, while the PDMS membrane was tested in 1 hour in CO_2 spiked water before it was moved back to tap water.

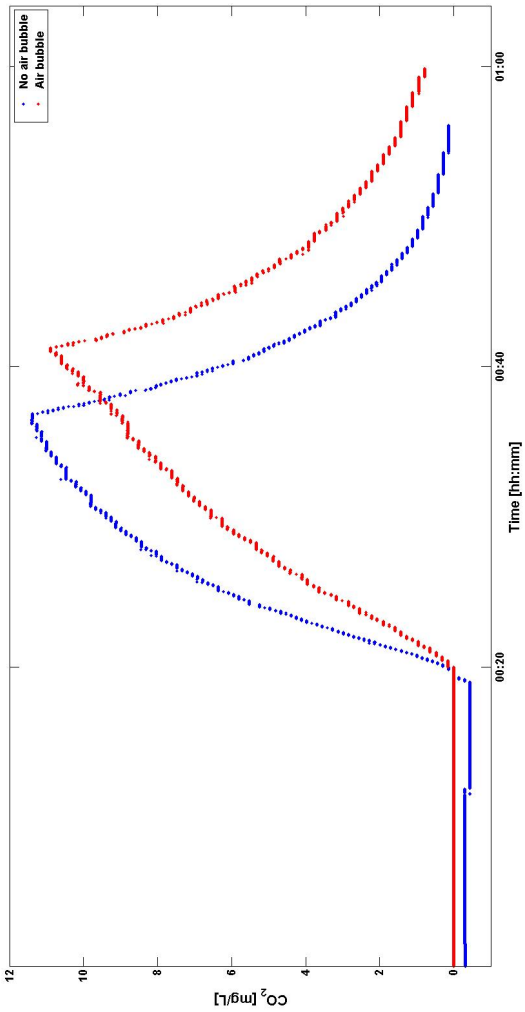

Figure A.5: Sensor readings using the open faced head with and without an air bubble accumulated on the membrane interface. The experiments were performed 10 minutes in tap water, 20 minutes in a spiked CO_2 solution, and lastly 20 minutes in tap water.

ii) Absorption of the PDMS membrane

Weight of the PDMS based membrane before and after 2 weeks in water, and the difference between them are shown in Table A.1.

Weight gain = 0.0031/0.5182 $\cdot$ 100 % = 0.6 %.

Table A.1: Weight before and after 2 weeks in water of the PDMS based membrane, and the difference between them.

Weight before	Weight after	Weight difference
0.5182 g	0.5213 g	0.0031 g

B Measurements at Nofima

i) Carbon dioxide calculations and measurements with Franatech probe

Results from measurements with the Franatech probe can be seen in Table B.1 In addition, CO_2 determined from total inorganic carbon (TIC), pH, temperature, salinity and experimentally determined dissociation constants are shown in the same table.

Table B.1: Results from the Franatech measurements, CO_{2F}, and CO_2 calculation, CO_{2Calc}. *No measurements due to Easter

Week	Date	Temperature [°C]	Vpm [μatm]	CO_{2F} [mg/L]	CO_{2Calc} [mg/L]
9	26.02.2019	10.5	3230	7.3	5.6
10	06.03.2019	10.2	2850	6.5	5.6
11	14.03.2019	11.2	2750	6.1	3.7
12	20.03.2019	11.1	2880	6.4	3.5
13	28.03.2019	11.3	2880	6.4	3.1
14	04.04.2019	11.3	3160	7.0	3.6
15	09.04.2019	11.1	3440	7.6	3.4
16*	-	-	-	-	-
17	26.04.2019	11.6	3720	8.1	5.3
18	02.05.2019	11.4	3655.7	8.0	3.2

ii) Example calculation of CO_2

An example calculation to determine CO_2 is shown below for S=13 ppt, T=12 °C, pH=7 and TIC=20 mg/L. ρ is 998 g/L. Molar mass of carbon is 12.0107 g/mole.

$$pK_1 = -8.712 - 9.460 \cdot 10^{-3} \cdot 13 + 8.56 \cdot 10^{-5} \cdot 13^2 + \frac{1355.1}{12 + 273.15} + 1.7976 \cdot ln(12 + 273.15) = 6.09 mol/kg \tag{B.1}$$

$$pK_2 = 17.0001 - 0.01259 \cdot 13 - 7.9334 \cdot 10^{-5} \cdot 13^2 + \frac{936.291}{12 + 273.15} - 1.87354 \cdot ln(12 + 273.15) - \frac{2.61471 \cdot 13}{12 + 273.15} + \frac{0.07479 \cdot 13^2}{12 + 273.15} = 9.44 mol/kg \tag{B.2}$$

$$K_1 = 10^{-\frac{6.09 \cdot 1000}{998}} = 7.84 \cdot 10^{-7} \tag{B.3}$$

$$K_2 = 10^{-\frac{9.44 \cdot 1000}{998}} = 3.47 \cdot 10^{-10} \tag{B.4}$$

$$[HCO_3^-] = \frac{20/12.0107}{\frac{10^{-7}}{7.9 \cdot 10^{-7}} + \frac{3.5 \cdot 10^{-10}}{10^{-7}} + 1} = 1.47 mmol/L \tag{B.5}$$

$$c_{CO_2} = \frac{10^{-7} \cdot 1.45}{7.9 \cdot 10^{-7}} \cdot 44.01 = 8.3 mg/L \tag{B.6}$$

iii) Result from classical titration

The standardization of the sodium hydroxide (NaOH) solution 06.03.2019 is shown in Table B.2, and the results from the classical carbon dioxide (CO_2) titration 08.03.2019 are shown in Table B.3. The blank is subtracted from the calculated NaOH and CO_2 concentrations.

Table B.2: Results from standardization of NaOH solution 06.03.2019.

Parallel	**KHP** [g]	**NaOH** [mL]	**NaOH** [mol/L]
Blank	-	0.10	-
1	0.1930	54.40	0.01737
2	0.2167	60.40	0.01757
3	0.1854	51.95	0.01746
Average	-	-	0.01747

Table B.3: Results from classical titration of CO_2 08.03.2019.

Parallel	**NaOH** [mL]	**CO_2** [mg/L]
Blank	0	0.10
1	4.80	9.0
2	4.65	8.7
3	4.70	8.8
Average	-	8.8

The standardization of the sodium hydroxide solution 21.03.2019 is shown in Table B.4, and the results from the classical CO_2 titration 22.03.2019 are shown in Table B.5.

Table B.4: Results from standardization of NaOH solution 21.03.2019.

Parallel	**KHP** [g]	**NaOH** [mL]	**NaOH** [mol/L]
Blank	-	0.10	-
1	0.2218	61.80	0.01763
2	0.1704	47.55	0.01762
3	0.1996	55.60	0.01764
Average	-	-	0.01763

Table B.5: Results from classical titration of CO_2 22.03.2019.

Parallel	**NaOH** [mL]	**CO_2** [mg/L]
Blank	0.30	-
1	4.70	8.5
2	4.70	8.5
3	4.60	8.3
Average	-	8.4

The standardization of the sodium hydroxide solution 08.04.2019 is shown in Table B.4, and the results from the classical CO_2 titration 10.04.2019 are shown in Table B.7.

Table B.6: Results from standardization of NaOH solution 08.04.2019.

Parallel	**KHP** [g]	**NaOH** [mL]	**NaOH** [mol/L]
Blank	0	0.20	-
1	0.1960	47.60	0.02025
2	0.1927	47.10	0.02012
3	0.1874	45.80	0.02012
Average	-	-	0.02016

Table B.7: Results from classical titration of CO_2 10.04.2019.

Parallel	**NaOH** [mL]	**CO_2** [mg/L]
Blank	0.30	-
1	4.00	8.2
2	4.00	8.2
3	3.90	8.0
Average	-	8.1

The standardization of the sodium hydroxide solution 26.04.2019 is shown in Table B.8, and the results from the classical CO_2 titration 25.04.2019 are shown in Table B.9.

Table B.8: Results from standardization of NaOH solution 26.04.2019.

Parallel	**KHP** [g]	**NaOH** [mL]	**NaOH** [mol/L]
Blank	0	0.10	-
1	0.1874	45.60	0.02008
2	0.2024	49.30	0.02006
3	0.1832	44.80	0.02007
Average	-	-	0.02007

Table B.9: Results from classical titration of CO_2 25.04.2019.

Parallel	**NaOH** [mL]	**CO_2** [mg/L]
Blank	0.30	-
1	4.50	9.3
2	4.30	8.8
3	3.40	9.0
Average	-	9.0

The standardization of the sodium hydroxide solution 07.05.2019 is shown in Table B.10, and the results from the classical CO_2 titration 08.05.2019 are shown in Table B.11.

Table B.10: Results from standardization of NaOH solution 07.05.2019.

Parallel	**KHP** [g]	**NaOH** [mL]	**NaOH** [mol/L]
Blank	-	0.10	-
1	0.1852	40.70	0.02233
2	0.1909	42.00	0.02231
3	0.1943	42.00	0.02270
Average	-	-	0.02245

Table B.11: Results from classical titration of CO_2 08.05.2019.

Parallel	**NaOH** [mL]	**CO_2** [mg/L]
Blank	0.40	-
1	4.20	9.4
2	4.10	9.1
3	4.00	8.9
Average	-	9.1

iv) Example calculation from NaOH standardization and CO_2 titration

The concentration of the NaOH solution was determined as shown in Equation (B.7).

$$c_{NaOH} = \frac{\frac{m_{KHP}}{M_{KHP}}}{V_{NaOH} - V_{blank}} = \frac{\frac{0.1930g}{204.22g/mol}}{0.05440L - 0L} = 0.1737mol/L \tag{B.7}$$

The concentration of carbon dioxide in mg/L in the sample was determined as shown below.

$$\begin{aligned} c_{CO_2} &= \frac{c_{NaOH} \cdot (V_{NaOH} - V_{blank}) \cdot M_{CO_2} \cdot 1000}{V_{sample}} \\ &= \frac{0.01737mol/L \cdot (4.80 - 0.10)mL \cdot 44.01g/mol \cdot 1000}{200mL \cdot 2} = 9.0mg/L \end{aligned} \tag{B.8}$$

Molar mass of potassium hydrogen phthalate (KHP) and CO_2 are shown in Table B.12.

Table B.12: Molar mass of CO_2 and potassium hydrogen phthalate (KHP). (Blackman, 2014)

Compound	**Molar mass** [g/mol]
CO_2	44.01
KHP	204.22

v) Open faced head

Enlarged version of the variation of carbon dioxide concentration over a two week period measured with the open faced head with error bars of $\pm$ 1 standard deviation showing every 7th hour is presented in Figure B.1. The event when sedimentation in the bucked was removed is shown in Figure B.2.

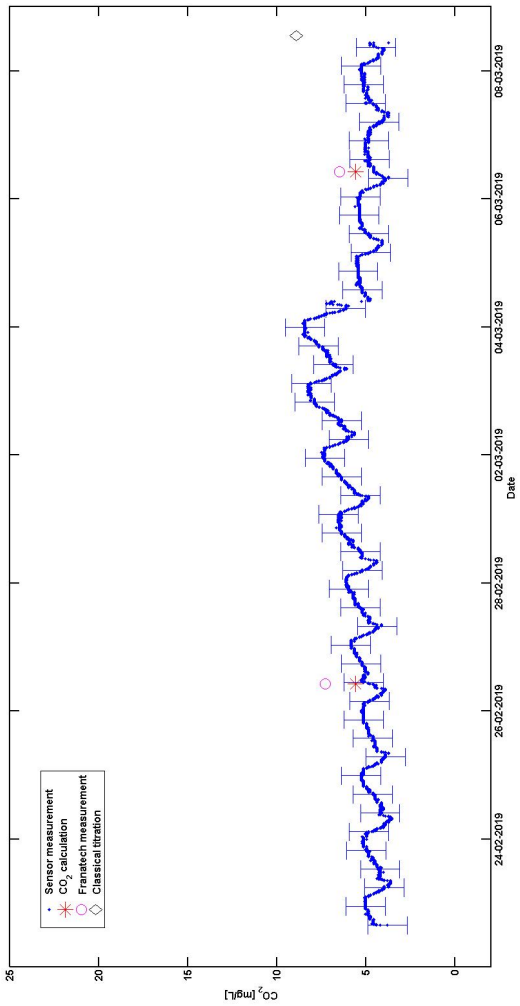

Figure B.1: Variation of carbon dioxide concentration over a two week period measured with the open faced head with error bars of $\pm$ 1 standard deviation showing every 7th hour. The red crosses are CO_2 concentrations calculated from TIC, salinity, temperature and pH measurements, the magenta circles are CO_2 measurements with the Franatech probe and the black diamond is the result from the classical titration with sodium hydroxide.

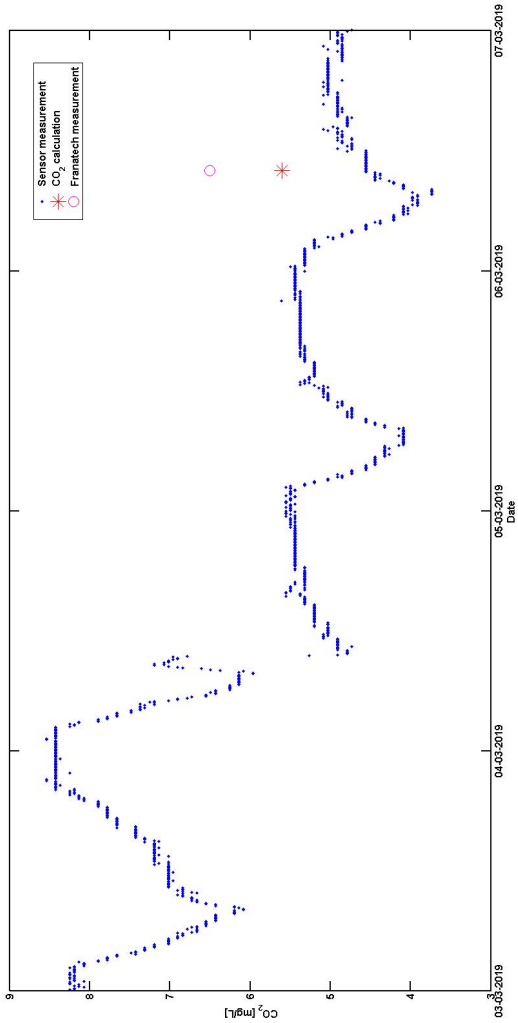

Figure B.2: The event when sedimentation were removed from the bucked when measuring with the open faced head. The red cross is CO_2 concentration calculated from TIC, salinity, temperature and pH measurements and the magenta circle is CO_2 measurement with the Franatech probe.

vi) Friedman test

The normality test of all 14 days showed non normal distribution. In Table B.13, the results from pairwise comparison from the Friedman test are shown for the open faced head. The Friedman test gave, χ^2 (13) = 2777, p $>$ 0.05. The mean rank of the days were 1.95, 2.27, 3.98, 5.36, 8.52, 10.03, 11.05, 12.05, 13.25, 13.54, 7.83, 6.65, 2.72 and 5.9 for day 1 to 14 respectively. The days with adj. sign $<$ 0.05 are shown below.

Table B.13: Results from Friedman pairwise comparison of days with open faced head showing for pair of days having adj. sign $<$ 0.05.

Pair of days	Adj. Sig
1 - 2	1.000
1 - 13	1.000
2 - 13	1.000
3 - 13	0.115
4 - 14	1.000
4 - 12	0.093
12 - 14	1.000
11 - 12	0.224
5 - 11	1.000
6 - 7	0.842
7 - 8	0.974
8 - 9	0.204
9 - 10	1.000

vii) Pumped head, copper grid and PDMS membrane

Enlarged versions of the variation of carbon dioxide concentration over a two week period with the water-pumped flow-through head, copper grid an PDMS membrane are shown in Figure B.3, Figure B.4 and Figure B.5 respectively.

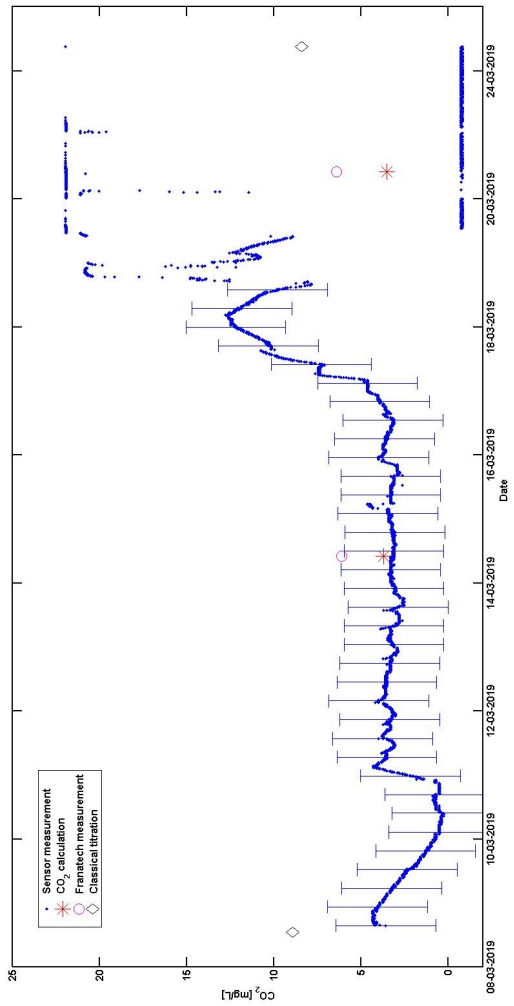

Figure B.3: Variation of carbon dioxide concentration over a two week period with the water-pumped flow-through head. Error bars of $\pm$ 1 standard deviation are drawn every 7th hour. The red crosses are CO_2 concentrations calculated from TIC, salinity, temperature and pH measurements, the magenta circles are CO_2 measurements with the Franatech probe and the black diamonds are results from the classical titration with sodium hydroxide.

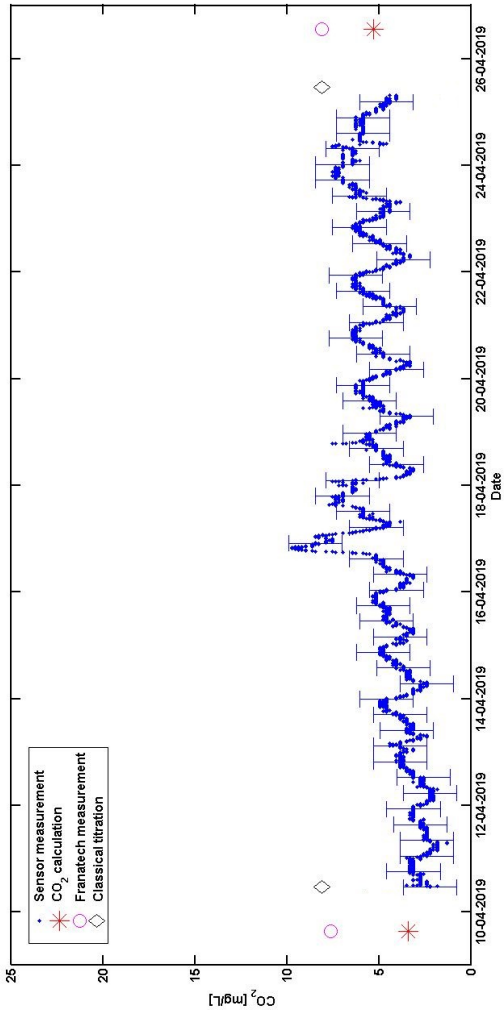

Figure B.4: Variation of carbon dioxide concentration over a two week period measured with the copper grid. Error bars of $\pm$ 1 standard deviation are showing every 7th hour. The red crosses are CO_2 concentrations calculated from TIC, salinity, temperature and pH measurements, the magenta circles are CO_2 measurements with the Franatech probe and the black diamond is the result from the classical titration with sodium hydroxide.

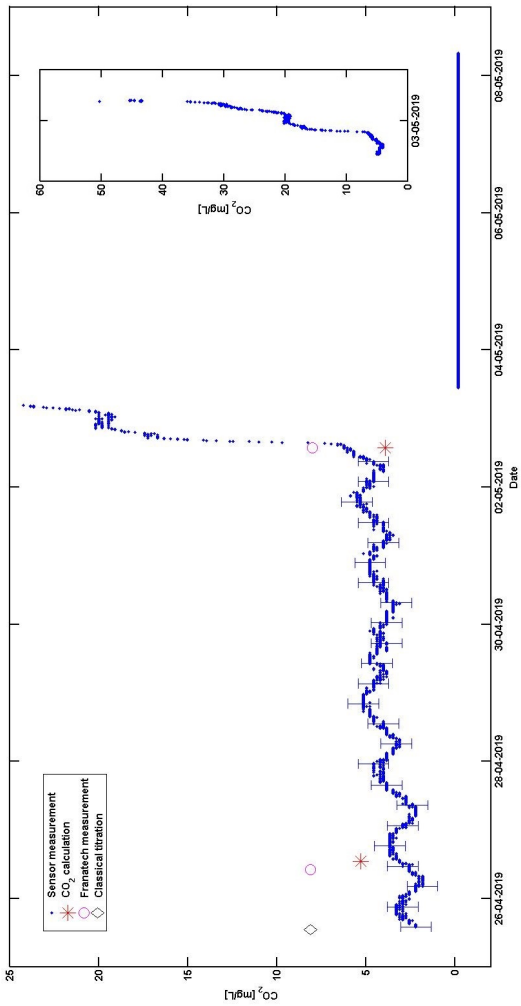

Figure B.5: Variation of carbon dioxide concentration over a two week period measured with the PDMS membrane together with the Teflon membrane. Error bars of $\pm$ 1 standard deviation are drawn every 7th hour. The red crosses are CO_2 concentrations calculated from TIC, salinity, temperature and pH measurements, the magenta circles are CO_2 measurements with the Franatech probe and the black diamonds are the result from the classical titration with sodium hydroxide.

viii) Estimate daily carbon dioxide increase

The daily carbon dioxide increase was calculating using Equation (B.9) and the following input data. Feed ingestion ratio was 25 kg feed/day, oxygen feed ratio was 0.25 kg O_2/ kg feed, the peaking factor was assumed to be 1, the water flow was 3600 m^2/day.

$$CO_2increase = \frac{PF \cdot FIR \cdot OFR \cdot 1.375 \cdot 1000}{V}$$
$$= \frac{1 \cdot 25kgfeed/day \cdot 0.25kgO_2/kgfeed \cdot 1.375 \frac{kgCO_2}{kgO_2} \cdot 1000}{3600m^3/day} = 2.4mg/L \quad \text{(B.9)}$$

ix) Comparative measurements

CO_2 concentrations calculated from TIC, pH, temperature (T) and salinity (S) of samples collected at 08:00, 10:00, 12:00, 14:00 and 16:00 the same day can be seen in Table B.14. The 3 first TIC samples were analyzed right after collection, TIC_{0h}, in addition to after 24 hours, TIC_{24h}, which resulted in CO_{20h} and CO_{224h}.

Table B.14: CO_2 concentrations calculated form TIC, pH, temperature (T) and salinity (S) values of samples collected at 08:00, 10:00, 12:00, 14:00 and 16:00 the same day. The 3 first TIC samples were analyzed right after collection, TIC_{0h} in addition to after 24 hours, TIC_{24h} which resulted in CO_{20h} and CO_{224h}.

Sample	**Collection** [hh:mm]	**pH**	**T** °C	**S** [ppt]	**TIC**$_{0h}$ [mg/L]	**TIC**$_{24h}$ [mg/L]	**CO2**$_{0h}$ [mg/L]	**CO2**$_{24h}$ [mg/L]
1	08:00	7.30	11.6	12.2	23.7	20.6	5.3	4.6
2	10:00	7.27	11.6	12.2	24.2	20.9	5.8	5.0
3	12:00	7.25	11.6	12.3	24.7	21.0	6.1	5.2
4	14:00	7.24	11.6	12.3	-	21.3	-	5.4
5	16:00	7.23	11.6	12.3	-	21.5	-	5.6

The carbon dioxide concentration variation through 24 hours for all four antifouling mechanism is presented in Figure B.6.

The original data and polynomial model plotted together for the open faced head, copper grid, pumped head and PDMS membrane can be seen in Figure B.7, Figure B.8, Figure B.9 and Figure B.10 respectively. The polynomial curve fittings for the four data sets are presented in **??**. Concentration of CO_2 during the incident when water penetrated behind the sensor membrane when using the pumped head and PDMS membrane can be seen in Figure B.12.

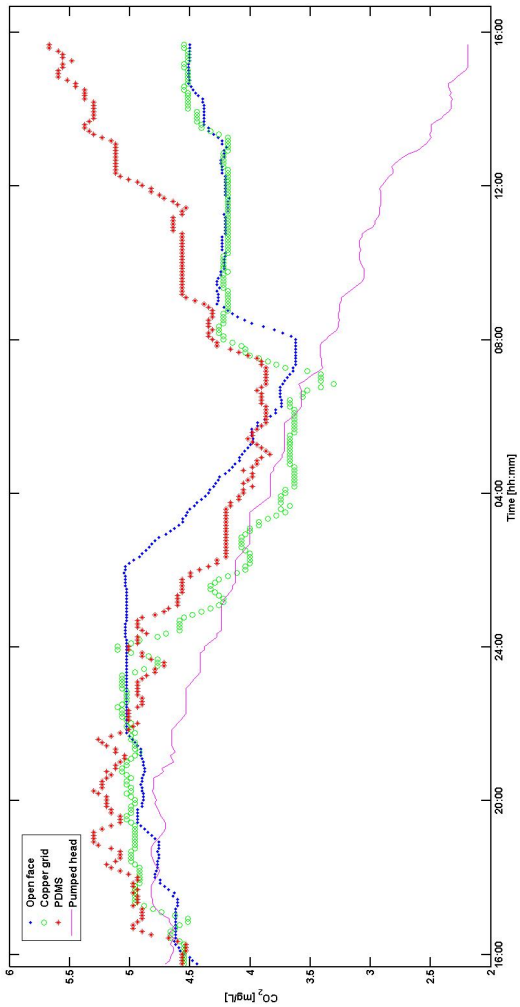

Figure B.6: The carbon dioxide concentration variation through 24 hours from day 1 and 7 with the open faced head.

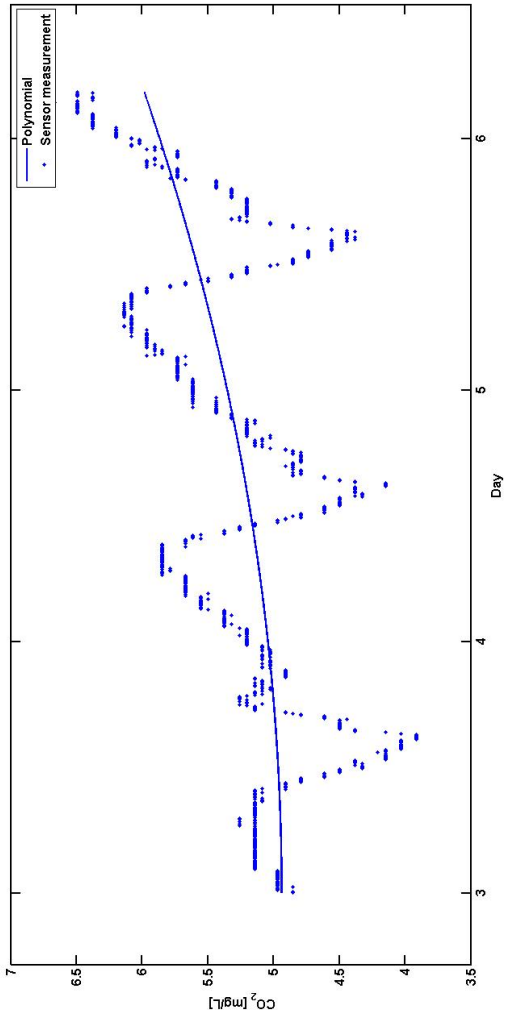

Figure B.7: Original data and polynomial model plotted together for the open faced head.

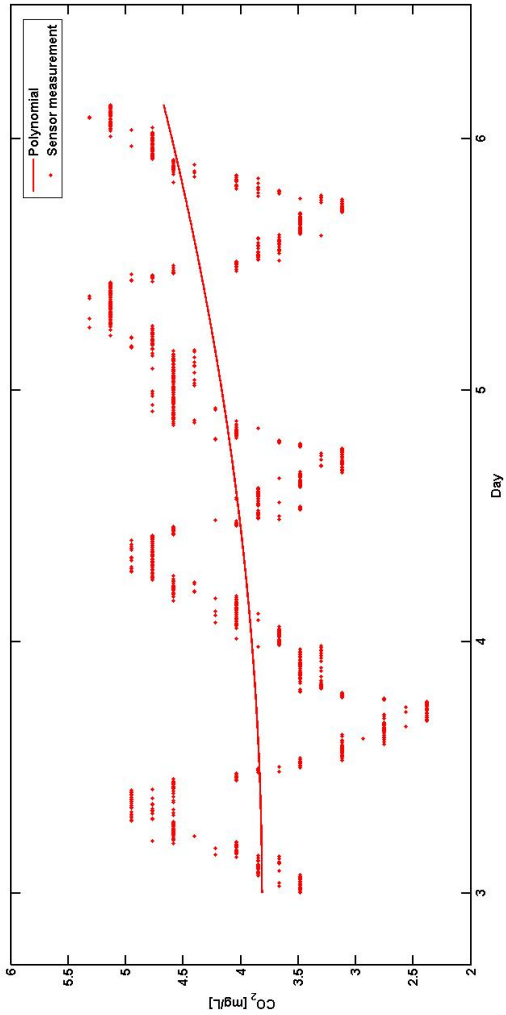

Figure B.8: Original data and polynomial model plotted together for the copper grid.

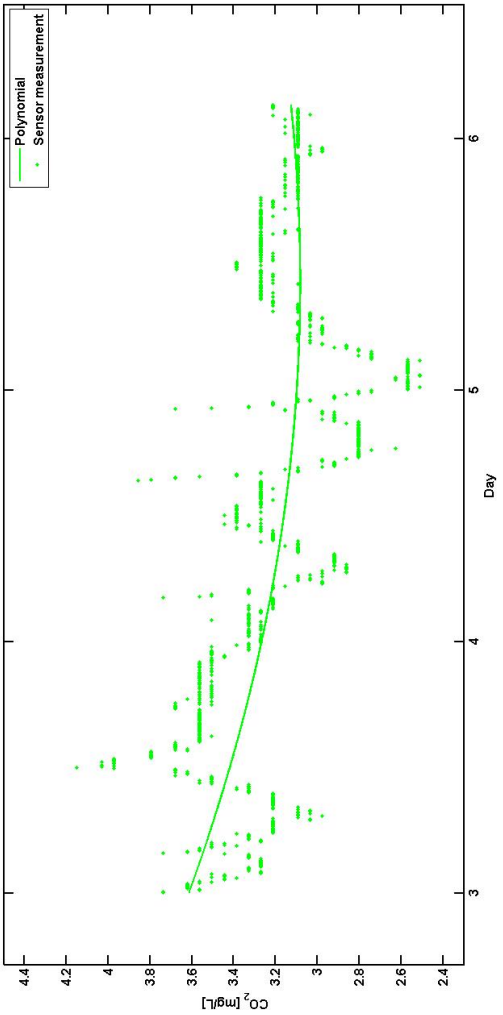

Figure B.9: Original data and polynomial model plotted together for the pumped head.

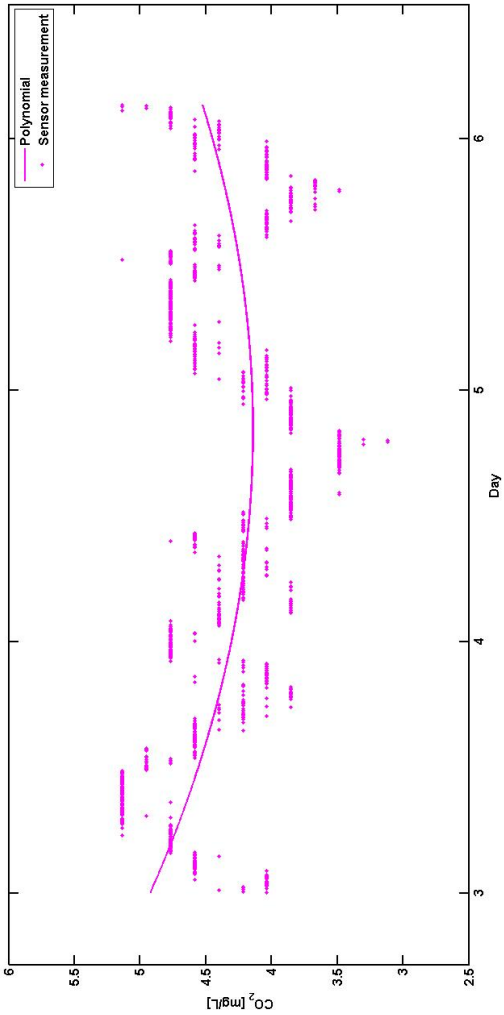

Figure B.10: Original data and polynomial model plotted together for the PDMS membrane.

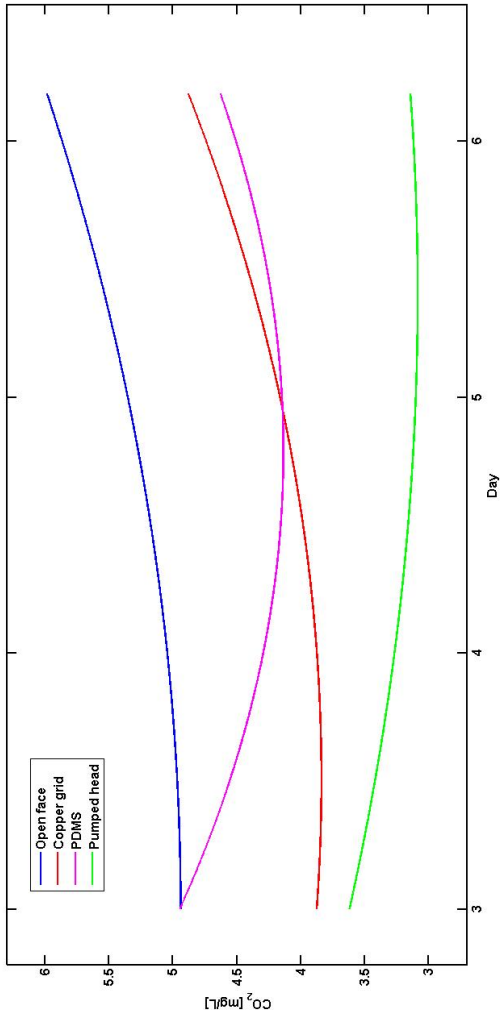

Figure B.11: Polynomial curve fitting of second degree for the four data sets. The blue, red, magenta and green line correspond to the curve of open face, copper grid, PDMS membrane and pumped head respectively.

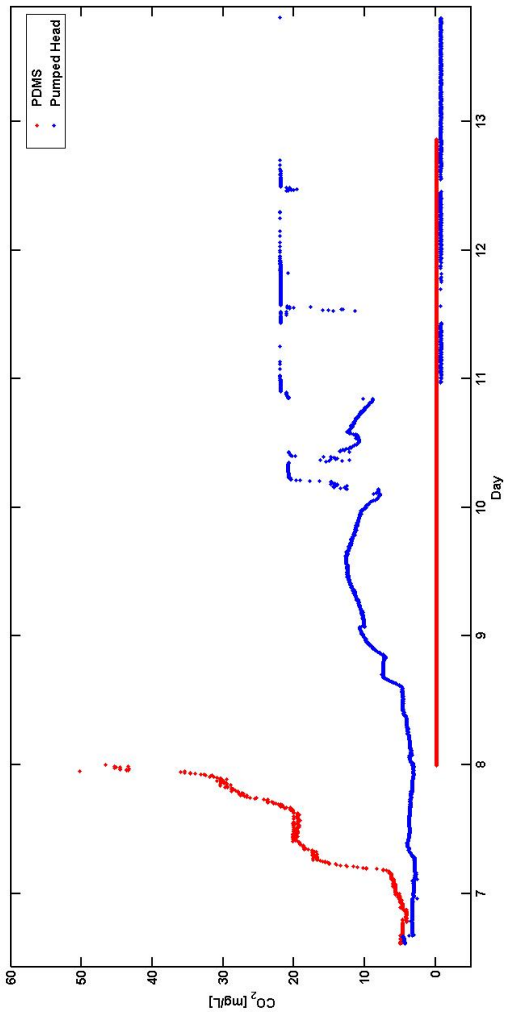

Figure B.12: Concentration of CO_2 during the incident when water penetrated behind the sensor membrane when using the pumped head and PDMS membrane.

C Matlab Code

Below is an example of the Matlab code used to plot the measurements. In this example the two week carbon dioxide measurements with the open faced head were plotted.

```
%%Plot measurements with open face head

%Create date string with dd-mmm-yyyy hh:mm:ss
expression = '\.';
replace = '\';
dateStr_OF = regexprep(Openface_Date,expression,replace);
dateTimeStr_OF = strcat(dateStr_OF,{' '},Openface_Time);
DateNum_OF = datenum(dateTimeStr_OF);

figure
hold on
%Plot measurement data
plot(DateNum_OF,Openface,'.')


%Plot reference samples
plot(datenum('02/26/2019 10:00'),5.6,'r*','markersize',18)  %CO2calc
plot(datenum('02/26/2019 10:00'),7.3,'mo','markersize',13)  %Franatech
plot(datenum('03/08/2019 13:00'),8.9,'dk','markersize',13)  %Titrering
plot(datenum('03/06/2019 10:00'),5.6,'r*','markersize',18)  %CO2calc
plot(datenum('03/06/2019 10:00'),6.5,'mo','markersize',13)  %Franatech

%Add errorbars every 7th hour
errorbar(DateNum_OF(1:84:length(Openface)),
    Openface(1:84:length(Openface)),
    ones(1,length(Openface(1:84:length(Openface)))) *std(Openface),'.')

%Settings
datetick('x','dd-mm-yyyy','keeplimits')
xlabel('Date','fontsize',12,'fontweight','bold');
ylabel('CO_2 [mg/L]','fontsize',12,'fontweight','bold');
set(gca,'fontsize',12,'fontweight','bold','linewidth',1.5);
legend('Sensor measurement','CO_2 calculation','Franatech measurement');
hold off
```

Listing C.1: Matlab code for plotting the two weeks carbon dioxide measurements with the open faced head.

The Matlab code used for creating the polynomial curve fitting is presented in Listing C.2.

```
%%%Polynomial curve fitting
hold on

%Open face
y1_OF = Openface(883:1785);
x1_OF = [883:1785]';
[p_OF, S_OF] = polyfit(x1_OF, y1_OF, 2);
y2_OF = polyval(p_OF,x1_OF);
plot(x1_OF,y2_OF,'linewidth',1.5)
%plot(x1_OF,y1_OF,'.');
MaxErr_OF = max(abs(y2_OF - y1_OF));

%Copper grid
y1_CG = CopperGrid(883:1785);
x1_CG= [883:1785]';
[p_CG, S_CG] = polyfit(x1_CG, y1_CG, 2);
y2_CG = polyval(p_CG,x1_CG);
plot(x1_CG,y2_CG,'r','linewidth',1.5)
%plot(x1_CG,y1_CG,'r.');
MaxErr_CG = max(abs(y2_CG - y1_CG));


%PDMS membrane
y1_PDMS = PDMS(883:1785);
x1_PDMS = [883:1785]';
[p_PDMS, S_PDMS] = polyfit(x1_PDMS, y1_PDMS, 2);
y2_PDMS = polyval(p_PDMS,x1_PDMS);
plot(x1_PDMS,y2_PDMS,'m','linewidth',1.5)
%plot(x1_PDMS,y1_PDMS,'m.')
MaxErr_PDMS = max(abs(y2_PDMS - y1_PDMS));

%Pumped head
y1_PH = PumpedHead(883:1785);
x1_PH = [883:1785]';
[p_PH, S_PH] = polyfit(x1_PH, y1_PH, 2);
y2_PH = polyval(p_PH,x1_PH);
plot(x1_PH,y2_PH,'g','linewidth',1.5)
%plot(x1_PH,y1_PH,'g.')
MaxErr_PH = max(abs(y2_PH - y1_PH));

%Settings
xlabel('Day','fontsize',12,'fontweight','bold'); ylabel('CO_2
    [mg/L]','fontsize',12,'fontweight','bold')
set(gca,'fontsize',12,'fontweight','bold','linewidth',1.5)
legend('Open faced head','Copper grid', 'PDMS', 'Pumped head')
hold off
```

Listing C.2: Matlab code for creating the polynomial curve fitting.

The Matlab code used to plot the daily variation is shown in Listing C.3.

```
%%Plot daily variation

%%Plot data using the smooth function
hold on
plot(smooth(Openface(198:485)),'.')          %start 15:30
plot(smooth(CopperGrid(58:345)+1.8),'og')    %start 15:29
plot(smooth(PDMS(79:366)+2),'r*')            %start 15:31
plot(smooth(PumpedHead(27:314)+0.5),'m-')    %start 15:27
hold off

%%Settings
xlabel('','fontsize',12,'fontweight','bold'); ylabel('CO_2
    [mg/L]','fontsize',12,'fontweight','bold')
set(gca,'fontsize',12,'fontweight','bold','linewidth',1.5)
legend('Open face','Copper grid','PDMS','Pumped head')
```

Listing C.3: Matlab code for daily variation of carbon dioxide concentration

Caroline Berge Hansen

Master's thesis

NTNU
Norwegian University of
Science and Technology